

# Odd Yao-Yao Graphs may Not be Spanners

Yifei Jin\*, Jian Li† and Wei Zhan‡

Tsinghua University, Beijing 100084, China

## Abstract

It is a long standing open problem whether Yao-Yao graphs  $YY_k$  are all spanners. Bauer and Damian [4] showed that all  $YY_{6k}$  for  $k \geq 6$  are spanners. Li and Zhan [21] generalized their result and proved that all even Yao-Yao graphs  $YY_{2k}$  are spanners (for  $k \geq 42$ ). However, their technique cannot be extended to odd Yao-Yao graphs, and whether they are spanners are still elusive. In this paper, we show that, surprisingly, for any integer  $k \geq 1$ , there exist odd Yao-Yao graph  $YY_{2k+1}$  instances, which are not spanners.

## 1 Introduction

Let  $\mathcal{P}$  be a set of points on the Euclidean plane  $\mathbb{R}^2$ . The complete Euclidean graph defined on set  $\mathcal{P}$  is the graph with vertex set  $\mathcal{P}$  and edges connecting all pairs of  $\mathcal{P}$ , where the weight of the edge is the Euclidean distance between its two end points. How to use a sparse subgraph to approximate the complete Euclidean graph is a classical problem in computational geometry [1, 17, 24, 30, 32]. In particular, it is desirable to obtain a  $t$ -spanner of bounded-degree (see e.g., [27]).

**Definition 1.** (Bounded Degree Spanner) A graph  $G$  is a bounded-degree geometric  $t$ -spanner of the complete Euclidean graph, if (1)  $G$  is a subgraph of the complete Euclidean graph; (2) the degree of any point is bounded by a constant number  $k$ , and (3) for any pair of points  $p$  and  $q$  in  $\mathcal{P}$ , the shortest path between  $p$  and  $q$  in  $G$  is no longer than  $t$  times the Euclidean distance between  $p$  and  $q$ .

The constant  $t$  is called *stretch factor* or *dilation factor* of the spanner in the literature. The concept of geometric spanners was first proposed by L.P. Chew [9]. See the comprehensive survey of Eppstein and David [14] for the related topics about geometric spanners. The geometric spanners have found a lot of applications in wireless ad hoc and sensor networks. We refer the readers to the books by Li [22] and Narasimhan and Smid [25] for more details.

*Yao graphs* are one of the first approximations of the complete Euclidean graph, introduced independently by Flinchbaugh and Jones [16] and Yao [32].

**Definition 2.** (Yao Graph  $Y_k$ )  $k$  is a fixed integer. Given a set of points  $\mathcal{P}$  be a set of points on the Euclidean plane  $\mathbb{R}^2$ , the Yao graph  $Y_k(\mathcal{P})$  is defined as follows. Let  $C_u(\gamma_1, \gamma_2]$  be the cone with apex  $u$ , which consists of the rays with polar angles in the half-open interval  $(\gamma_1, \gamma_2]$ . For each point  $u \in \mathcal{P}$ ,  $Y_k(\mathcal{P})$  contains the edge connecting  $u$  to the nearest neighbor  $v$  in each cone  $C_u(j\theta, (j+1)\theta]$ , for  $\theta = 2\pi/k$  and  $j \in [0, k-1]$ . We generally refer Yao graphs as undirected graphs. For directed Yao graph, we add the directed edge  $\overrightarrow{uv}$  to the graph instead.

---

\*jin-yf13@mails.tsinghua.edu.cn

†lijian83@mail.tsinghua.edu.cn

‡zhanw-13@mails.tsinghua.edu.cn

Molla [13] showed that  $Y_2$  and  $Y_3$  may not be spanners, but  $Y_k$  for  $k \geq 4$  are all spanners. Bose et al. [6] proved that  $Y_4$  is a 663-spanner. Barba et al. [2] showed that  $Y_5$  is a 3.74-spanner. Damian and Raudonis [12] proved that  $Y_6$  graph is a 17.64 spanner. Li et al. [23, 24] first proved that all  $Y_k, k > 6$  are spanners with stretch factor at most  $1/(1 - 2 \sin(\pi/k))$ . Later Bose et al. [6, 7] also obtained the same result independently. Recently, Barba et al. [2] improved the stretch factor to  $1/(1 - 2 \sin(3\pi/4k))$  for odd  $k \geq 7$ .

However, Yao graphs may not have a bounded degree. It is a serious limitation in certain wireless network applications since each node has very limited energy and communication capacity, and can only communicate with a small number of neighbors. To address the issue, Li et al. [24] introduced *Yao-Yao* graphs (or *Sparse-Yao* graphs in the literature). A Yao-Yao graph  $YY_k(\mathcal{P})$  is obtained by removing some edges from  $Y_k(\mathcal{P})$  as follows:

**Definition 3.** (*Yao-Yao Graphs  $YY_k$* ) (1) Construct the directed Yao graph, as in Definition 2. (2) For each node  $u$  and each cone rooted at  $u$  containing two or more incoming edges, retain the shortest incoming edge and discard the rest. We can see that the maximum degree in  $YY_k(\mathcal{P})$  is upper-bounded by  $2k$ .

Different from Yao graphs, the spanning property of Yao-Yao graphs is still not well understood yet. Li et al. [24] provided some empirical evidence, suggesting that  $YY_k$  graphs are  $t$ -spanners for  $k$  being a sufficiently large constant. However, there is no theoretical proof yet, and it is still an open problem [4, 21, 22, 24]. It is also listed as Problem 70 in the Open Problems Project.<sup>1</sup>

**Conjecture 1.** *There exists a constant  $k_0$  such that for any integer  $k > k_0$ , any Yao-Yao graph  $YY_k$  is a geometric spanner.*

Now, we briefly review the previous results about Yao-Yao graphs. It is known that  $YY_2$  and  $YY_3$  may not be spanners since  $Y_2$  and  $Y_3$  may not be spanners [13]. Damian and Molla [11, 13] proved that  $YY_4, YY_6$  may not be spanners. Bauer et al. [2] proved that  $YY_5$  may not be spanners. On the positive side, Bauer and Damian [4] showed that for any integer  $k \geq 6$ , any Yao-Yao graph  $YY_{6k}$  is a spanner with stretch factor 11.67 and the factor becomes to 4.75 for  $k \geq 8$ . Recently, Li and Zhan [21] proved that for any integer  $k \geq 42$ , any even Yao-Yao graph  $YY_{2k}$  is a spanner with stretch factor  $6.03 + O(k^{-1})$ .

From these positive results, it is quite attempting to believe Conjecture 1. However, we show in this paper that, surprisingly, Conjecture 1 is false for odd Yao-Yao graphs.

**Theorem 4.** *For any  $k \geq 1$ , there exists a class of instances  $\{\mathcal{P}_m\}_{m \in \mathbb{Z}^+}$  such that the stretch factor of  $YY_{2k+1}(\mathcal{P}_m)$  cannot be bounded by any constant, as  $m$  approaches infinity.*

**Related Work** It has been proven that in some special cases, the Yao-Yao graphs are spanners [10, 19, 20, 31]. Specifically, it was showed that  $YY_k$  graphs are spanners in *civilized graph*, where the distance between any two nodes in this graph is larger than a constant  $\lambda$  [19, 20].

Besides Yao and Yao-Yao graph, another common geometric  $t$ -spanner is called  $\Theta$ -graph. The difference between  $\Theta$ -graphs and Yao graphs is that in a  $\Theta$ -graph, the neighbor nearest to  $u$  in a cone  $C$  is a point lying in  $C$  and minimizing the Euclidean distance between  $u$  and the orthogonal projection of  $v$  onto the bisector of  $C$ . It is known that except  $\Theta_2$  and  $\Theta_3$  [13], for  $k = 4$  [3], 5 [8], 6 [5],  $\geq 7$  [26],  $\Theta_k$ -graphs are all geometric spanners. We note that, unfortunately, the degrees of  $\Theta$ -graphs may not be bounded.

Recently, some variants of geometric  $t$ -spanner such as weak  $t$ -spanner and power  $t$ -spanner have been studied. In the power  $t$ -spanner, the Euclidean distance  $|\cdot|$  is replaced by  $|\cdot|^\kappa$  with a constant  $\kappa \geq 2$ . Schindelbauer et al. [28, 29] proved that for  $k > 6$ , any Yao-Yao graphs  $YY_k$  are power  $t$ -spanners for some constant  $t$ . However, it is known that any  $t$ -spanner is also a weak  $t_1$ -spanner and a power  $t_2$ -spanner for appropriate  $t_1, t_2$  depending only on  $t$  and the converse is not true [29].

<sup>1</sup><http://cs.smith.edu/~orourke/TOPP/P70.html>

Fractals have been used to construct the examples for  $\beta$ -skeleton graphs with unbounded stretch factor [15]. Schindelbauer et al. [29] used the same example to prove that there exist graphs which are weak spanners but not  $t$ -spanners. However, their examples cannot serve as counterexamples for odd Yao-Yao graphs.

## 2 Overview of our Counterexample Construction

We first note that both the counterexamples for  $YY_3$  and  $YY_5$  are not weak  $t$ -spanners (in a weak  $t$ -spanner, the path between two points may be arbitrarily long, but must remain within a disk of radius  $t$ -times the Euclidean distance between the points). However, it is known that all Yao-Yao graphs  $YY_k$  for  $k \geq 7$  are weak  $t$ -spanners for some constant  $t$  [18, 28, 29]. Hence, to construct the counterexamples for  $YY_k$  for  $k \geq 7$ , the previous ideas for  $YY_3$  and  $YY_5$  cannot be used. We will construct a class of instance  $\{\mathcal{P}_m\}_{m \in \mathbb{Z}^+}$ , such that the length of the polygonal path diverges as  $m$  approaches infinity. Moreover, all points in our counterexample locate in a bounded area.

Our example contains two types of points, called *normal points* and *auxiliary points*. Denote them by  $\mathcal{P}_m^n$  and  $\mathcal{P}_m^a$  respectively and  $\mathcal{P}_m = \mathcal{P}_m^n \cup \mathcal{P}_m^a$ . The normal points form the basic skeleton, and the auxiliary points are used to break the edges connecting any two normal points that are far apart.

We are inspired by the concept of fractals to construct the normal points. A fractal can be contained in a bounded area, but its length may diverge. In our counterexample, through specifying the order of the points, the path between two specific normal points is a fractal-like polygonal path. Suppose the two specific points are  $\mu_1$  and  $\mu_2$ ,  $\mu_1\mu_2$  is horizontal, and  $|\mu_1\mu_2| = 1$ . When  $m = 0$ , the polygonal path is just the line segment  $\mu_1\mu_2$ . When  $m$  increases by one, we replace each line segment in the current polygonal path by a *sawteeth-like* path (see Figure 1a). It is not difficult to see that if we can continue this process, the length of the resulting path would increase to infinity as  $m$  approaches infinity. More specifically, if the angle between each segment of the sawteeth-like path and the base segment (i.e., the one which is replaced) is  $\gamma$ , the total length of the path increase by a factor of  $\cos^{-1} \gamma$ . An important observation here is that the factor is independent of the number of sawteeth (see Figure 1b). However, we need to make sure that such a path is indeed in a Yao-Yao graph and it is indeed the shortest path from  $\mu_1$  to  $\mu_2$ . There are two technical difficulties we need to overcome.

1. As  $m$  increases, the polygonal path may intersect itself around the turning points (see Figure 1d for an example). This is relatively easy to handle: we do not recurse for those segments that may cause self-intersection (see Figure 1e). We need to make sure that the total length of such segments is proportionally small (so that the total length can keep increasing as  $m$  increases).
2. In the Yao-Yao graph defined over the normal points constructed in the recursion, there may be some edges connecting points that are far apart. Actually, how to break such edges is the main difficulty of the problem. We outline the main techniques as follows.

First, we *do not* replace all current segments using the same sawteeth, like in the usual fractal construction. Actually, for each segment, we will choose a specific path such that the paths have different numbers of sawteeth and the size of each sawtooth may not be same even in the same path. See Figure 1f. Finally, we construct them in a specific sequential order. Actually, we organize the normal points in an  $m$ -level *recursion tree*  $\mathcal{T}$  and generate them in the DFS preorder of the tree. We spell out the details in Section 3.

Second, we group the normal points into a collection of sets such that each normal point belongs to exactly one set. We call such a set a *hinge set*. Refer to Figure 12 for an overview. Then, we specify a total order of the hinge sets. Call the edges in the Yao-Yao graph  $YY_{2k+1}(\mathcal{P}_m^n)$  connecting any two points in the

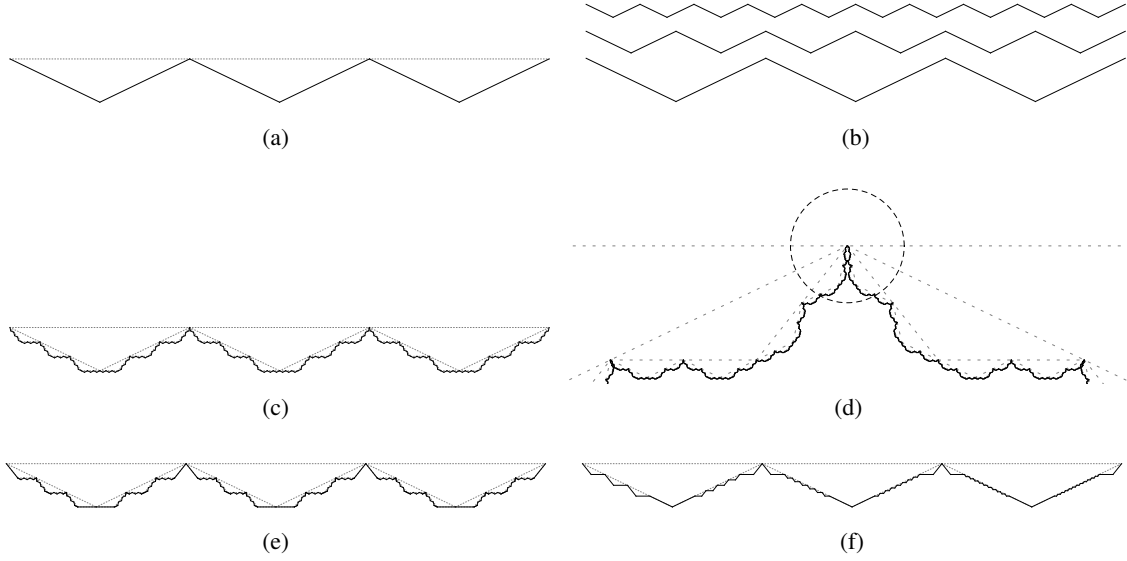


Figure 1: The fractal and its variants. In Figure 1a, we replace a horizontal segment by a sawteeth-like path. In Figure 1b, we illustrate that the lengths of the sawteeth-like paths are independent of the number of sawteeth. In Figure 1c, the polygonal path may intersect itself. Figure 1d is an enlarged view of Figure 1c around a turing point. In Figure 1e, we do not recurse for those segments that may cause self-intersection. In Figure 1f, paths have different numbers of sawteeth and the size of each sawtooth may not be same.

same hinge set or two adjacent hinge sets (w.r.t. the total order) *hinge connections* and call the other edges *long range connections*. We spell out the details in Section 4.

Geometrically, we will see that the all possible long range connections are relatively simple. Hence, we can break all long range connections by adding a set  $\mathcal{P}_m^a$  of *auxiliary points* (e.g., see Figure 23). Let the minimum distance between any two normal points in  $\mathcal{P}_m^n$  be  $\Delta$ . Each auxiliary point  $q$  is centered on a normal point  $p$  such that  $|pq|$  is much less than  $\Delta$ . Naturally, we can generalize the concepts hinge set and long range connection to include the auxiliary points. An *extended hinge set* consists of the normal points in a hinge set and the auxiliary points centered on these normal points. We will see that the auxiliary points break all long range connections and introduce no new long range connection. We spell out the details in Section 5.

Finally, according to the process above, we can see that the shortest path between the normal points  $\mu_1$  and  $\mu_2$  in  $\mathcal{Y}\mathcal{Y}_{2k+1}(\mathcal{P}_m)$  for  $m \in \mathbb{Z}^+$  should pass through all extended hinge sets in order. Thereby, the length of the shortest path between  $\mu_1$  and  $\mu_2$  diverges as  $m$  approaches infinity. We spell out the details in Section 6.

### 3 The Positions of Normal Points

In this section, we describe the positions of normal points. We need to introduce a few notions first. In this section, we only care about the positions of the points. The segments in any figure of this section are used to illustrate the relative positions of the points. Those segments may not represent the edges in Yao or Yao-Yao graphs. See Figure 2 for an overview of the positions of the normal points.

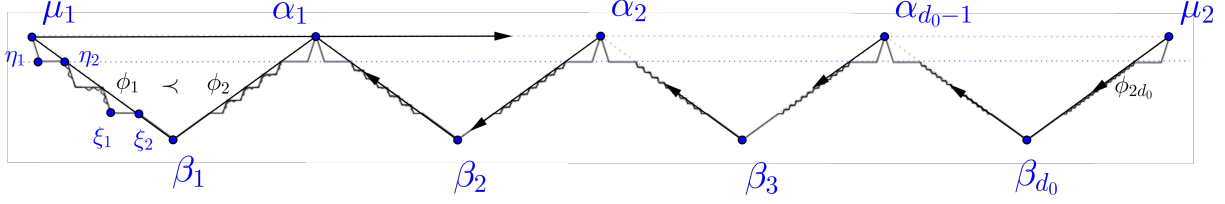


Figure 2: The overview of the positions of the normal points.  $\mu_1\mu_2$  is horizontal.  $\{\alpha_1, \alpha_2, \dots, \alpha_{d_0-1}\}$  partitions the segment  $\mu_1\mu_2$  into  $d_0$  equal parts. For each  $\beta_i$ ,  $\angle\alpha_{i-1}\beta_i\alpha_i = \pi - \theta$  and  $|\alpha_{i-1}\beta_i| = |\beta_i\alpha_i|$ . We call  $\{\alpha_1, \alpha_2, \dots, \alpha_{d_0-1}\}$  the partition set and  $\{\beta_1, \beta_2, \dots, \beta_{d_0}\}$  the apex set of pair  $(\mu_1, \mu_2)$ .

### 3.1 Some Basic Concepts

Let  $k \geq 3$  be a fixed positive integer. We consider  $\mathbb{Y}\mathbb{Y}_{2k+1}$  and let  $\theta = 2\pi/(2k+1)$ .

**Definition 5** (Cone Boundary). Consider any two points  $u$  and  $v$ . If the polar angle of  $\vec{uv}$  is  $j\theta = j \cdot 2\pi/(2k+1)$  for some  $j \in [2k+1]$ , we call the ray  $\vec{uv}$  a cone boundary for point  $u$ .

Note that in an odd Yao-Yao graph, if  $\vec{uv}$  is a cone boundary, its reverse  $\vec{vu}$  is not a cone boundary. In retrospect, this property is a key difference between odd Yao-Yao graphs and even Yao-Yao graphs, and our counterexample for odd Yao-Yao graphs will make crucial use of the property. We make it explicit as follows.

**Property 6.** Consider two points  $u$  and  $v$  in  $\mathcal{P}$ . If  $\vec{uv}$  is a cone boundary in  $\mathbb{Y}\mathbb{Y}_{2k+1}(\mathcal{P})$ , its reverse  $\vec{vu}$  is not a cone boundary.

**Definition 7** (Pair). A pair is two ordered points, denoted by  $(w_1, w_2)$ , such that  $\vec{w_1w_2}$  is a cone boundary of point  $w_1$ .

Note that a pair is two *ordered* points. According to Property 6, if  $(w_1, w_2)$  is a pair, its reverse  $(w_2, w_1)$  is not a pair. Moreover, if a pair  $\phi$  is  $(u, \cdot)$  or  $(\cdot, u)$ , we say that the point  $u$  belongs to  $\phi$  (i.e.,  $u \in \phi$ ).

**Gadget:** Now, we introduce the concept of a gadget generated by a pair  $\phi = (w_1, w_2)$ . Such a gadget is a collection of points which is a superset of  $\phi$  (see Figure 3). If the recursive level  $m$  increases by 1, we use a gadget generated by pair  $\phi$  to replace  $\phi$ .

One gadget  $G_\phi$  consists of three groups of points. We explain them one by one. See Figure 3 for an example.

1. The first group is the pair  $\phi = (w_1, w_2)$ . We call the pair the *generating-pair* or the *parent-pair* of the gadget  $G_\phi$ .
2. The second group is a set  $\mathcal{A}_\phi$  of points on the segment of  $(w_1, w_2)$ . We call the set  $\mathcal{A}_\phi$  a *partition set* and call the points of  $\mathcal{A}_\phi$  the *partition points* of  $\phi$ . For example, in Figure 3,  $\{\alpha_1, \alpha_2, \dots, \alpha_7\}$  (here,  $|w_1\alpha_i| < |w_1\alpha_j|$  if  $i < j$ ) is a partition set of  $(w_1, w_2)$ . The set  $\mathcal{A}_\phi$  divides the segment into  $|\mathcal{A}_\phi| + 1$  parts, each we call a *piece* of the segment.
3. There are two types of pieces. One is called an *empty piece* and the other a *non-empty piece*. Whether a piece is empty or not is determined in the process of the construction, which we will explain in Section 3.3. For each non-empty piece, e.g.,  $\alpha_{i-1}\alpha_i$ , we add a point  $\beta_i$  such that  $\angle\alpha_{i-1}\beta_i\alpha_i = \pi - \theta$  and  $|\alpha_{i-1}\beta_i| = |\beta_i\alpha_i|$ .<sup>2</sup> All  $\beta_i$ s are on the same side of  $w_1w_2$ . We call such a point  $\beta_i$  an *apex point*

<sup>2</sup>Note that the subscript  $i$  of  $\beta_i$  is consistent with the subscript of the piece  $\alpha_{i-1}\alpha_i$ . Hence, the subscripts may not be consecutive among all  $\beta_i$ s.

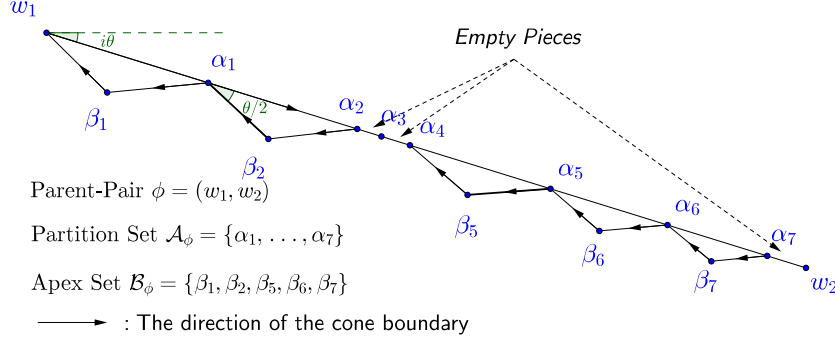


Figure 3: An example of one gadget.  $\phi = (w_1, w_2)$  is the parent-pair in the gadget.  $\mathcal{A}_\phi = \{\alpha_1, \alpha_2, \alpha_3, \dots, \alpha_7\}$  is the partition set and  $\mathcal{B}_\phi = \{\beta_1, \beta_2, \beta_5, \beta_6, \beta_7\}$  is the apex set. There are eight pieces, in which  $w_1\alpha_1, \alpha_1\alpha_2, \alpha_4\alpha_5, \alpha_5\alpha_6, \alpha_6\alpha_7$  are non-empty pieces and  $\alpha_2\alpha_3, \alpha_3\alpha_4, \alpha_7w_2$  are empty pieces.

of  $(w_1, w_2)$ . Let  $\mathcal{B}_\phi = \{\beta_i\}_i$ , which we call the *apex set* of pair  $(w_1, w_2)$ .  $\mathcal{B}_\phi$  is the third group of points. In Figure 3,  $\{\beta_1, \beta_2, \beta_5, \beta_6, \beta_7\}$  is an apex set of  $(w_1, w_2)$ .

We summarize the above construction in the following definition.

**Definition 8 (Gadget).** A gadget  $G_\phi$  generated by a pair  $\phi$  is a set of points which consists of the pair  $\phi$ , a partition set  $\mathcal{A}_\phi$  and an apex set  $\mathcal{B}_\phi$  of  $\phi$ . We denote the gadget by  $G_\phi[\mathcal{A}_\phi, \mathcal{B}_\phi]$ .

Consider a gadget  $G_\phi[\mathcal{A}_\phi, \mathcal{B}_\phi]$ , where  $\phi = (w_1, w_2)$ . For any non-empty piece  $\alpha_{i-1}\alpha_i$  and the corresponding apex point  $\beta_i$ , it is easy to check that the rays  $\overrightarrow{\beta_i\alpha_{i-1}}$  and  $\overrightarrow{\alpha_i\beta_i}$  (note the order of the points) are cone boundaries. Thus, each point  $\beta_i \in \mathcal{B}_\phi$  induces two pairs  $(\beta_i, \alpha_{i-1})$  and  $(\alpha_i, \beta_i)$ . We call all pairs  $(\beta_i, \alpha_{i-1})$  and  $(\alpha_i, \beta_i)$  induced by points in  $\mathcal{B}_\phi$  the *child-pairs* of  $(w_1, w_2)$ , and we say that they are *siblings* of each other. Now, we define the order of the child-pairs of pair  $(w_1, w_2)$ , based on their distances to  $w_1$ . Here, the distance from a point  $w$  to a pair  $\phi$  is the shortest distance from  $w$  to any point of  $\phi$ .

**Definition 9 (The Order of the Child-pairs).** Consider a gadget  $G_{(w_1, w_2)}$ . Suppose  $\Phi$  is the set of the child-pairs of  $(w_1, w_2)$ . Consider two pairs  $\phi, \varphi$  in  $\Phi$ . Define the order  $\phi \prec \varphi$ , if  $\phi$  is closer to  $w_1$  than  $\varphi$ .

For example, in Figure 3,  $(\beta_2, \alpha_1) \prec (\alpha_5, \beta_5)$ . We emphasize that the order of the child-pairs is related to the direction of their parent-pair.

### 3.2 The Recursion Tree

As we mentioned before, our goal is to construct an  $m$ -level tree. When the recursion level increases by 1, we need to replace each current pair by a gadget generated by the pair. The recursion can be naturally represented as a tree  $\mathcal{T}$ . Each node of the tree represents either a pair or a point. To avoid confusion, we use *point* to express a point in  $\mathbb{R}^2$  and *node* to express a vertex in the tree. The pair  $(\mu_1, \mu_2)$  is the root of the tree (*level-0*). The child-pairs of  $(\mu_1, \mu_2)$  are the child-nodes of the root (they are at *level-1*). Recursively, each child-pair of a pair  $\phi$  is a child-node of the node  $\phi$  in  $\mathcal{T}$ . Besides, there are some *partition points* of the empty pieces (e.g., the point  $\alpha_3$  in Figure 4) which may not belong to any pair. Let such an *isolated* partition point be a leaf in  $\mathcal{T}$  and the parent of such a *point* be its generating pair. For example, the parent of  $\alpha_3$  is the pair  $(w_1, w_2)$  in Figure 4. We provide the recursion tree in Figure 5, which is corresponding the points in Figure 4.

The nodes with the same parent are siblings. According to Definition 9, we define a total order “ $\prec$ ” of them. We note that here “ $\varphi \prec \phi$ ” does not mean that  $\varphi$  is on the left hand side of  $\phi$  geometrically. For



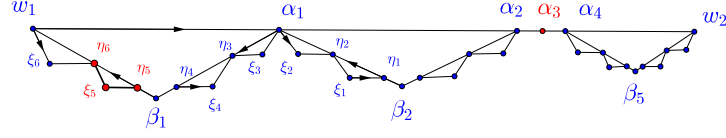


Figure 4: An example of the gadgets which are generated in a recursive manner.  $\alpha_3$  is an isolated partition point. The arrow of a segment indicates the order of two points in the pair. For example, the arrow from  $w_1$  to  $w_2$  indicates that  $(w_1, w_2)$  is a pair.

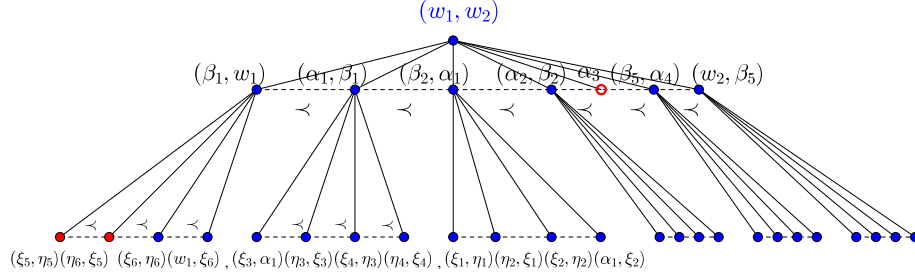


Figure 5: The recursion tree of our construction. Each node of the tree represents a pair (e.g.,  $(\beta_1, w_1)$ ) or a point (e.g.,  $\alpha_3$ ), which is corresponding to the pair or the point in Figure 4. Regard pair  $(w_1, w_2)$  as the root at level-0. Any pair at level- $(i + 1)$  is generated from a pair at level- $i$ .

---

**Algorithm 1:** GenGadget( $\phi$ ): Generate the Normal Points in  $\mathcal{T}_\phi$

---

```

1 if  $\phi$  is a leaf-pair then
2   | Return ;
3 else
4   |  $G_\phi \leftarrow \text{Proj-Refn}(\phi)$ ;
5 foreach child-pair  $\varphi$  of  $\phi$  do
6   | GenGadget( $\varphi$ ) ;

```

---

example, in Figure 4, pair  $(\xi_5, \eta_5) \prec (\eta_6, \xi_5)$  in the tree  $\mathcal{T}$ , but in the Euclidean plane, point  $\eta_5$  is on the right side of  $\eta_6$ .

For a pair  $\phi$  (corresponding to a node in  $\mathcal{T}$ ), we use  $\mathcal{T}_\phi$  to denote the subtree rooted at  $\phi$  (including  $\phi$ ), or all the points involved in the subtree.

Our counterexample  $\mathcal{P}_m$  corresponds to a recursion tree with  $m$  levels. We have not yet specified how to choose the partition set for each gadget and decide which pieces are empty for each pair. We will do it in the next subsection. We note that we *do not* construct the tree level by level, but rather according to the DFS preorder.

### 3.3 The Construction

Now, we describe the process of generating the  $m$ -level recursion tree  $\mathcal{T}$ . The tree is generated according to the DFS preorder, starting from the root. When we are visiting a pair, we generate its gadget. Note that generating its gadget is equivalent to generating its children in  $\mathcal{T}$  (we, however, do not visit those children during the generation. They will be visited later according to the DFS preorder). See Figure 6 for an example.

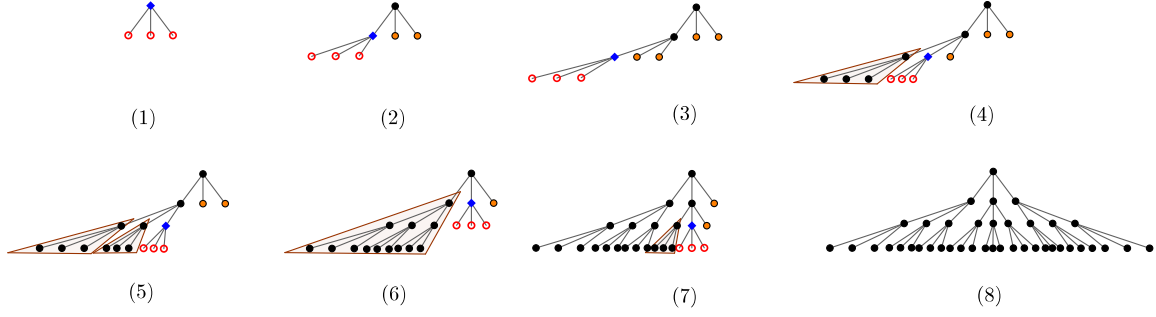


Figure 6: The process of generating a tree according to the DFS preorder. This is just a diagram to illustrate the steps of the generation process. In each subfigure,  $\blacklozenge$  represents a node we are visiting. The nodes generated in the step are denoted by  $\circ$ .  $\bullet$  represents a node which has already been visited.  $\bullet$  represents a node which has been created but not been visited yet. The nodes covered by light brown triangles are related to the process projection.

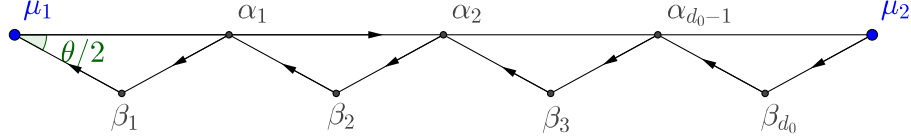


Figure 7: The root gadget  $G_\phi(\mathcal{A}_\phi, \mathcal{B}_\phi)$  where  $\phi = (\mu_1, \mu_2)$ .  $\mu_1\mu_2$  is horizontal.  $\mathcal{A}_\phi$  is the equidistant partition. Each piece is non-empty.

The root of  $\mathcal{T}$  is the pair  $(\mu_1, \mu_2)$  and we assume without loss of generality that  $\mu_1\mu_2$  is horizontal. We call a pair a *leaf-pair* if it is a leaf node in the tree and an *internal-pair* otherwise. Note that not all leaf-pairs are at *level-m*. Whether a pair is a leaf or not is determined when the gadget is created.

Each time when we visit an internal-pair, we use a process called *projection and refinement* to generate its gadget. We denote the procedure by  $\text{GenGadget}(\phi)$  and the pseudocode can be found in Algorithm 1. We generate the pairs according to the DFS preorder.

**Root gadget:** Consider a pair  $(\mu_1, \mu_2)$ . Let  $\mathcal{A}_\phi$  be its partition set which contains points

$$\alpha_i = \mu_1 \cdot \frac{d_0 - i}{d_0} + \mu_2 \cdot \frac{i}{d_0}, i \in [1, d_0 - 1].$$

For convenience, let  $\alpha_0 = \mu_1, \alpha_{d_0} = \mu_2$ .  $\{\alpha_i\}_i$  partitions the segment  $\mu_1\mu_2$  into  $d_0$  pieces with equal length  $|\mu_1\mu_2|/d_0$ . All pieces in the root gadget are non-empty. For each piece  $\alpha_{i-1}\alpha_i$ , we add an apex point  $\beta_i$  below  $\mu_1\mu_2$ . Let  $\mathcal{B}_\phi$  be the apex set. See Figure 7 for an example.

Then, we discuss the process *projection and refinement*. For convenience, we say that the *segment of a pair* is the segment connecting the two points of the pair and the *length of a pair* is the length of that segment. In the process, we always keep the property as follows.

**Property 10.** Consider an internal-pair  $\phi$ . Suppose  $\varphi$  is one sibling of  $\phi$ . The length of pair  $\varphi$  is at least half of the length of pair  $\phi$ .

**Projection and Refinement:** The projection and refinement process for  $\phi$  is slightly more complicated, as



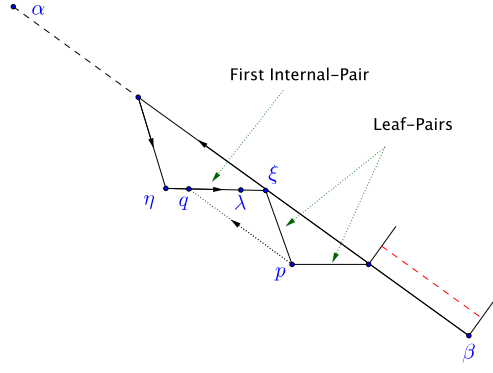


Figure 8: An example of the projection for the first internal-pair  $\phi = (\eta, \xi)$ . First, we add a point  $\lambda$  such that  $|\lambda\xi| = \delta/d_0$  where  $\delta$  is the length  $|\eta\xi|$ . Second, for each leaf-pair  $\varphi \prec \phi$ , project its apex point  $p$  to the segment of  $\phi$  along the direction  $\beta\alpha$ , i.e., add the point  $q$  in the figure.

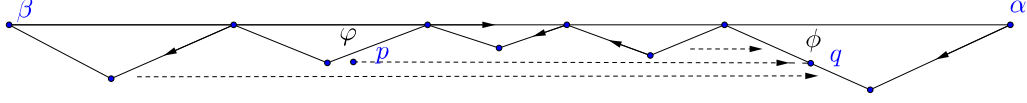


Figure 9: The projection for pair  $\phi$ . Here,  $p$  is a point in subtree  $\mathcal{T}_\varphi$ .  $q$  is a projection point of  $p$ , i.e, the point on segment of pair  $\phi$  such that  $pq$  is parallel to  $\beta\alpha$ . The set  $\text{Proj}[\bigcup_{\varphi \prec \phi} \mathcal{T}_\varphi]$  consists of all projection points of  $\bigcup_{\varphi \prec \phi} \mathcal{T}_\varphi$  on segment of  $\phi$ .

it depends on the subtrees  $\mathcal{T}_\varphi$  rooted at the siblings  $\varphi$  of  $\phi$  such that  $\varphi \prec \phi$ . Recall that when we visit a pair  $\phi$  (and generate  $G_\phi$ ) in the tree  $\mathcal{T}$  according to the DFS preorder, we have already visited all pairs  $\varphi \prec \phi$ .

– **Projection:** Consider a pair  $(\beta, \alpha)$  with the set  $\Phi$  of its child-pairs. We decide whether a pair in  $\Phi$  is a leaf-pair or not after introducing the process projection and refinement. Here, we claim that among the pairs in  $\Phi$ , there is no leaf-pair between two internal-pairs based on our construction. It means that for  $\phi_1, \phi_2, \phi_3 \in \Phi$ , if  $\phi_1 \prec \phi_2 \prec \phi_3$  and  $\phi_1$  and  $\phi_3$  are two internal-pairs, then  $\phi_2$  is an internal-pair. Besides, we define the first internal-pair in the direction  $\beta\alpha$  as the *first internal-pair* of  $\Phi$ .

Then, we apply the projection operation for a pair  $\phi \in \Phi$ . W.l.o.g, suppose  $\phi$  is an internal-pair since only internal-pairs have children.

- $\phi$  is the first internal-pair of  $\Phi$ : In Figure 8, pair  $(\eta, \xi)$  is the first internal child-pair of  $(\beta, \alpha)$ . Suppose the length of  $\phi$  is  $\delta$ .  $\xi \in \phi$  and  $\xi$  is a partition point. First, we add a point  $\lambda$  on the segment of  $\phi$  such that  $|\lambda\xi| = \delta/d_0$ . Second, for each leaf-pair  $\varphi \prec \phi$ , project the apex point in  $\varphi$  to segment the of  $\phi$  along the direction  $\beta\alpha$ . Note that the length of leaf-pair  $\varphi$  is at least  $\delta/2$  according to Property 10. Thus, there is no point between  $\lambda$  and  $\xi$ .
- $\phi$  belongs to the other internal-pairs: According to the DFS preorder, we have already constructed the subtrees rooted at  $\varphi \prec \phi$ . Let  $\mathcal{T}_\varphi$  be the set of points in the subtree rooted at  $\varphi$ . We project all points  $p \in \bigcup_{\varphi \prec \phi} \mathcal{T}_\varphi$  to the segment  $\phi$  along the direction  $\beta\alpha$ . Let the partition set  $\mathcal{A}_\phi$  of  $\phi$  be the set of the projected points. If more than one points overlap, we keep only one of them. See Figure 9 for an example.

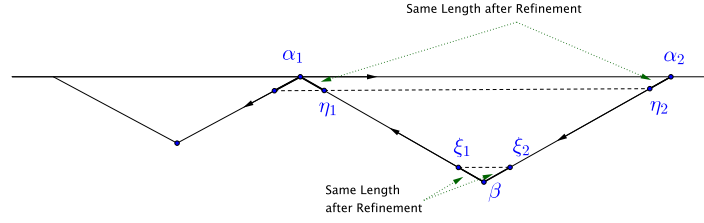


Figure 10: The two cases for refinement. The first case is  $(\beta, \alpha_1)$  in which the first point is an apex point. We mark the piece incident on  $\alpha_1$ , i.e., the piece  $\alpha_1\eta_1$ . The second case is  $(\alpha_2, \beta)$ , in which the first point is a partition point. We mark the two pieces incident on  $\alpha_2$  and  $\beta$  respectively, i.e., the pieces  $\alpha_2\eta_2$  and  $\xi_2\beta$ . Note that after refinement,  $|\beta\xi_1| = |\beta\xi_2|$  and  $|\alpha_1\eta_1| = |\alpha_2\eta_2|$  since there is no point added on the marked pieces after refinement.

We define such process as the *projection* operation and denote it by

$$\hat{\mathcal{A}}_\phi \leftarrow \text{Proj} \left[ \bigcup_{\varphi \prec \phi} \mathcal{T}_\varphi \right]. \quad (1)$$

– **Refinement:** The partition points of  $\phi$  divide the segment of  $\phi$  into pieces. In order to keep Property 10, we need to ensure that all non-empty pieces of  $\phi$  have approximately the same length. We call such process the *refinement* operation. After the projection, we obtain a candidate partition set  $\hat{\mathcal{A}}_\phi$  of  $\phi$  (defined in (1)). However, note that the length between the pieces may differ a lot. Let  $|\hat{\mathcal{A}}_\phi| = n$ . If  $n \leq d_0$ , we further repeatedly split the inner pieces (i.e., all pieces except the two incident on the points of  $\phi$ ) into two equal-length pieces until the number of the points in  $\hat{\mathcal{A}}_\phi$  is larger than  $d_0$ . Thus, w.l.o.g., suppose pair  $\phi$  has unit length and  $|\hat{\mathcal{A}}_\phi| = n$  and  $n > d_0$ .

Suppose  $\phi = (u_1, u_2)$ . We divide into two cases based on whether the first point  $u_1$  is a partition point or an apex point.

- If  $u_1$  is an apex point, we mark the piece incident on  $u_2$  (e.g., piece  $\alpha_1\eta_1$  in Figure 10).
- If  $u_1$  is a partition point, we mark the pieces incident on  $u_1$  and  $u_2$  (e.g., piece  $\alpha_2\eta_2$  and  $\xi_2\beta$  in Figure 10).

Denote the lengths of  $i$ th piece (defined by  $\hat{\mathcal{A}}_\phi$ ) by  $\delta_i$ . Let  $\delta_o = 1/n^2$ . Except the marked piece(s), for each other piece which is at least twice longer than  $\delta_o$ , we place  $\lfloor \delta_i/\delta_o \rfloor - 1$  equidistant points on the piece, which divide the piece into  $\lfloor \delta_i/\delta_o \rfloor$  equal-length parts.

We call such process the *refinement* and denote the resulting point set by

$$\mathcal{A}_\phi \leftarrow \text{Refine}[\hat{\mathcal{A}}_\phi]. \quad (2)$$

The number of points which we add in the refinement process is at most  $O(n^2)$  since the segment of pair  $\phi$  has unit length and  $\delta_o \geq 1/n^2$ . We call each other piece whose length is less than  $\delta_o$  a *short piece*. The short pieces remain unchanged before and after the refinement. Moreover, the refinement does not introduce any new short piece for the pair.

**Deciding Emptiness:** Then, we discuss the principle to decide whether a piece is empty or non-empty. Consider a pair  $\phi$ . Suppose  $\beta$  is an apex point and  $\alpha$  is a partition point, and  $\beta$  and  $\alpha$  belong to  $\phi$ . We let the piece incident on the apex point  $\beta$  and the short pieces be empty and other pieces be non-empty.

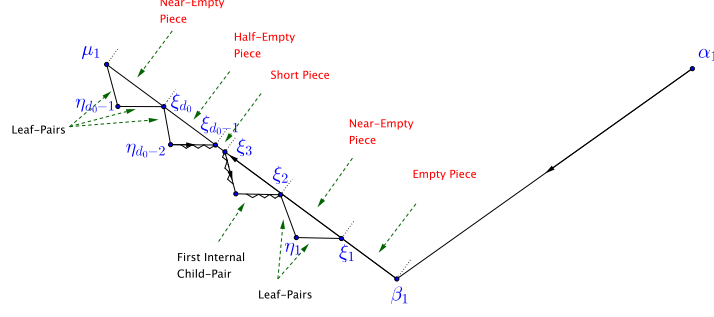


Figure 11: The figure illustrates the emptiness of each piece. Consider the pair  $(\beta_1 \mu_1)$  with partition points after refinement.  $\mu_1 \xi_{d_0}$  and  $\xi_1 \xi_2$  are two near-empty pieces and  $\beta_1 \xi_1$  is an empty piece.  $(\mu_1, \eta_{d_0-1})$  and  $(\eta_{d_0-1}, \xi_{d_0})$ ,  $(\xi_{d_0}, \eta_{d_0-2})$ ,  $(\xi_2, \eta_1)$ ,  $(\eta_1, \xi_1)$  are the five leaf-pairs.  $\xi_{d_0-1} \xi_{d_0}$  is the half-empty piece.  $(\xi_1, \eta_2)$  is the first internal-pair.

For each non-empty piece, we generate one apex point. As we discuss before, the apex set  $\mathcal{B}_\phi$  induces the set  $\Phi$  of child-pairs of  $\phi$ . Let the three pairs closest to  $\alpha$  and two pairs closest to  $\beta$  be *leaf-pairs*. We do not further expand the tree from the leaf-pairs. Let other pairs be the *internal-pairs*. For convenience, we call the piece generating two leaf-pairs a *near-empty piece* and generating one leaf-pair and one internal-pair a *half-empty piece*. See Figure 11 for an example. Note that the near-empty and half-empty pieces are special non-empty pieces.

We can see that except the near-empty piece incident on the partition point in  $\phi$  (e.g.,  $\mu_1 \xi_{d_0}$  in Figure 11), the maximum length among the non-empty pieces is at most twice longer than the minimum one according to refinement. After deciding emptiness, we can see that except the point in the root pair, each point belongs to at most two pairs. Moreover, there is no leaf-pair between any two internal-pairs among pairs in  $\Phi$ .

Overall, after the projection and refinement process, we can generate the gadget for any pair in the tree. We denote this process by

$$G_\phi \leftarrow \text{Proj-Refn}(\phi). \quad (3)$$

**Property 11.** Consider two sibling pairs  $\phi$  and  $\varphi$ . Suppose both of them are internal-pairs and have partition point sets  $\mathcal{A}_\phi$  and  $\mathcal{A}_\varphi$  respectively. Suppose  $\alpha_\phi \in \phi$  and  $\alpha_\varphi \in \varphi$ , and both  $\alpha_\phi$  and  $\alpha_\varphi$  are partition points. The point in  $\mathcal{A}_\phi$  closest to  $\alpha_\phi$  is  $v_\phi$ . Meanwhile, the point in  $\mathcal{A}_\varphi$  closest to  $\alpha_\varphi$  is  $v_\varphi$ . Then  $|\alpha_\phi v_\phi| = |\alpha_\varphi v_\varphi|$ .

*Proof.* W.l.o.g, we prove that any two adjacent siblings satisfy the property. Suppose  $\phi$  and  $\varphi$  are adjacent siblings. W.l.o.g, assume  $\varphi \prec \phi$ .  $\phi$  has the candidate partition set  $\hat{\mathcal{A}}_\phi$  after projection. Suppose the point in  $\hat{\mathcal{A}}_\phi$  closest to  $\alpha_\phi$  is  $\hat{v}_\phi$ . According to the projection, we know  $|\alpha_\phi \hat{v}_\phi| = |\alpha_\varphi v_\varphi|$ . Since we do not add any new point between  $\alpha_\phi \hat{v}_\phi$  after refinement,  $\hat{v}_\phi$  and  $v_\phi$  are the same point. Hence, any two adjacent siblings have the property.  $\square$

**Corollary 12.** Consider a pair  $\phi$  with partition point set  $\mathcal{A}_\phi$ . Suppose  $\alpha \in \phi$  and  $\alpha$  is a partition point. Among all pieces determined by  $\mathcal{A}_\phi$ , the piece incident on  $\alpha$  has the maximum length.

*Proof.* If  $\phi$  is the first internal-pair of its parent-pair, the corollary is trivially true according to the projection process (the first case projection). Otherwise, according to Property 11, it still has the maximum length.  $\square$

Now, we prove Property 10 that we claimed at the beginning of the construction.

*Proof of Property 10:* Consider an arbitrary pair with partition point  $\alpha$  and the set  $\Phi$  of its child-pairs. We prove that all its child-pairs satisfy Property 10. Hence, recursively, any internal-pair satisfies the property. Consider an internal-pair  $\phi \in \Phi$ . Note that the length of a child-pair is determined by its corresponding piece. According to the construction, except the near-empty piece incident on  $\alpha$ , the length of any non-empty piece is at most twice and at least half the length of another one. Thus, except the sibling pairs generated by the piece incident on  $\alpha$ , the length of any pair  $\varphi \prec \phi$  is at least half of the length of  $\phi$ . Finally, the piece incident on  $\alpha$  only induces two leaf-pairs and has maximum length among other empty pieces of  $\phi$  according to the Corollary 12. Hence, we have proven the property.  $\square$

Finally, we summarize the properties of half-empty, near-empty, and empty pieces as follows.

**Property 13.** *Consider an internal-pair  $\phi$  with partition point set  $\mathcal{A}_\phi$ . Suppose the length of  $\phi$  is  $\delta$ . The pieces determined by  $\mathcal{A}_\phi$  have the following properties.*

- *The sum of lengths of empty pieces is less than  $2\delta/d_0$ .*
- *There are two near-empty pieces with sum of lengths less than  $3\delta/d_0$ .*
- *There is one half-empty piece with length less than  $\delta/d_0$ .*
- *The sum of lengths of empty, near-empty and half-empty pieces is less than  $6\delta/d_0$ .*

*Proof.* Consider the first property. Suppose  $\beta \in \phi$  and  $\beta$  is an apex point. There are two kinds of empty pieces. One is the short pieces and the other is a piece incident on  $\beta$  (denoted by  $\xi\beta$ ). First, the sum of lengths of short pieces is less than  $\delta/d_0$ . Because the length of each short piece is less than  $\delta/n^2$  and there are less than  $n$  short pieces where  $n > d_0$  is the number of partition points in  $\hat{\mathcal{A}}$  after projection and before refinement. On the other hand, we prove that the length of  $\xi\beta$  is less than  $\delta/d_0$ . If  $\beta$  is the first point of  $\phi$ , according to refinement (first case for refinement), the length of  $\xi\beta$  is less than  $\delta/d_0$ . Then consider the case that  $\beta$  is the second point of  $\phi$ . Suppose  $\phi$  shares the point  $\beta$  with its sibling  $\varphi$ . Hence,  $\phi$  and  $\varphi$  share the point  $\beta$ . Denote the piece of  $\varphi$  incident on  $\beta$  by  $\eta\beta$ . In this case, we have that  $\phi$  and  $\varphi$  have the same length and  $|\xi\beta| = |\eta\beta|$ . Since  $\beta$  is the first point  $\varphi$ , we have  $|\eta\beta| \leq \delta/d_0$ . Thus,  $|\xi\beta| \leq \delta/d_0$ .

Consider the second property. Suppose  $\alpha$  is a partition point and  $\beta$  is an apex point, and  $\alpha, \beta \in \phi$ . First, consider the near-empty piece incident on  $\alpha$ . If  $\phi$  is the first internal-pair of its parent, according to projection, we add a point  $\lambda$  on the segment of  $\phi$  such that  $|\lambda\alpha| = \delta/d_0$ . Otherwise, according to Property 11 and 10, we know the piece incident on  $\alpha$  is at most  $2\delta/d_0$ . Second, we consider the other near-empty piece closer to  $\beta$ . Its length is no more than  $\delta/d_0$  based on refinement. Thus, the sum of lengths of near-empty pieces is less than  $3\delta/d_0$ .

For the third property, through refinement, it can be seen directly that the length of half-empty piece is less than  $\delta/d_0$ . Above all, we get the fourth property.  $\square$

## 4 Hinge Set Decomposition of the Normal Points

We have explained the positions of the normal points. Then, we discuss the edges among the normal points. For convenience, we regard the Yao-Yao graph as a directed graph. Recall the construction of the directed Yao-Yao graph in Algorithm 2. Note that  $C_u(\gamma_1, \gamma_2]$  represents the cone with apex  $u$  and consisting of the rays with polar angles in the half-open interval  $(\gamma_1, \gamma_2]$  in anticlockwise. We call the first iteration (line 2 to 5) the *Yao-step* and call the second iteration (line 6 to 9) the *Reverse-Yao step*.

Denote the set of normal points by  $\mathcal{P}_m^n$  where  $m$  is the level of the tree and  $n$  represents the word “normal”. In this section, we discuss the edges among normal points in  $\text{YY}_{2k+1}(\mathcal{P}_m^n)$ . There are two kinds of edges in the graph. One is called *long range connections* and the other *hinge connections*. See Figure 12 for an overview of the two kinds of edges. First, we decompose the point set into *hinge sets* and define a total

---

**Algorithm 2:** Construct the Yao-Yao graph
 

---

**Data:** A point set  $\mathcal{P}$  and an integer  $k \geq 2$

**Result:**  $YY_{2k+1}$  graph

```

1 Initialize:  $\theta = 2\pi/(2k+1)$  and two empty graphs  $Y_{2k+1}$  and  $YY_{2k+1}$  ;
2 foreach point  $u$  in  $\mathcal{P}$  do
3   foreach  $j$  in  $[0, 2k]$  do
4     Select  $v$  in  $C_u(j\theta, (j+1)\theta]$  such that  $|uv|$  is the shortest ;
5     Add edge  $\vec{uv}$  into  $Y_{2k+1}$ 
6 foreach point  $u$  in  $\mathcal{P}$  do
7   foreach  $j$  in  $[0, 2k]$  do
8     Select  $v$  in  $C_u(j\theta, (j+1)\theta]$ ,  $\vec{vu} \in Y_{2k+1}$  such that  $|uv|$  is the shortest ;
9     Add edge  $\vec{vu}$  into  $YY_{2k+1}$ 
10 return  $YY_{2k+1}$ 
  
```

---

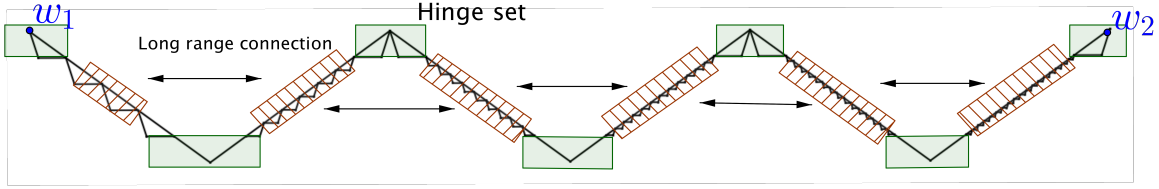


Figure 12: The overview of the hinge connections and long range connections. Roughly speaking, each set of points covered by a green rectangle  $\square$  is a hinge set. Recursively, we can further decompose the points covered by shadowed rectangle  $\boxtimes$  into hinge sets. The hinge connections are the edges between any two points in a hinge set or between two adjacent hinge sets. The other edges in the Yao-Yao graph are long range connections.

order among hinge sets. We call an edge between any two points in the same hinge set or in two adjacent hinge sets w.r.t. the total order *hinge connections*. Call other edges *long range connections*. In Section 5, we prove that we can break all long range connections without introducing new ones by adding some auxiliary points. In Section 6, we show that in the graph with hinge connections, the shortest path between the two points of the root pair approaches to infinity.

**Hinge connection:** Then we discuss the process to decompose the set  $\mathcal{P}_m^n$  into *hinge sets* such that each point in  $\mathcal{P}_m^n$  belongs to exactly one hinge set. Briefly speaking, each hinge set is a set of points which are close geometrically.

Consider a pair  $\hat{\phi}$  at level- $t$ ,  $t < m - 1$  with partition point set  $\mathcal{A}_{\hat{\phi}}$  and apex point set  $\mathcal{B}_{\hat{\phi}}$ . Denote the set of the child-pairs of  $\hat{\phi}$  by  $\hat{\Phi}$ .

- The hinge set centered on a point  $\beta \in \mathcal{B}_{\hat{\phi}}$ : Suppose  $\beta$  belongs to one or two internal-pairs in  $\hat{\Phi}$ , which we denote as  $\varphi$  and  $\phi$ .<sup>3</sup> The hinge set centered  $\beta$  includes:  $\beta$  itself, the child-pair of  $\varphi$  closest to  $\beta$  (i.e.,  $(\xi_1, \xi_2)$  in Figure 13a) and the child-pair of  $\phi$  closest to  $\beta$  (i.e.,  $(\eta_1, \eta_2)$  in Figure 13a). Note that  $\xi_1, \xi_2, \eta_1, \eta_2$  are only incident on leaf-pairs. Otherwise, if  $\beta$  is incident on two leaf-pairs, there is no hinge set centered on  $\beta$ . Actually,  $\beta$  belongs to hinge set centered on the points of  $\hat{\phi}$ .

---

<sup>3</sup>  $\beta$  must belong to two child-pairs of  $\hat{\phi}$  since each  $\beta$  induces two pairs. If one of the two child-pairs is a leaf-pair, let  $\varphi = \emptyset$ .

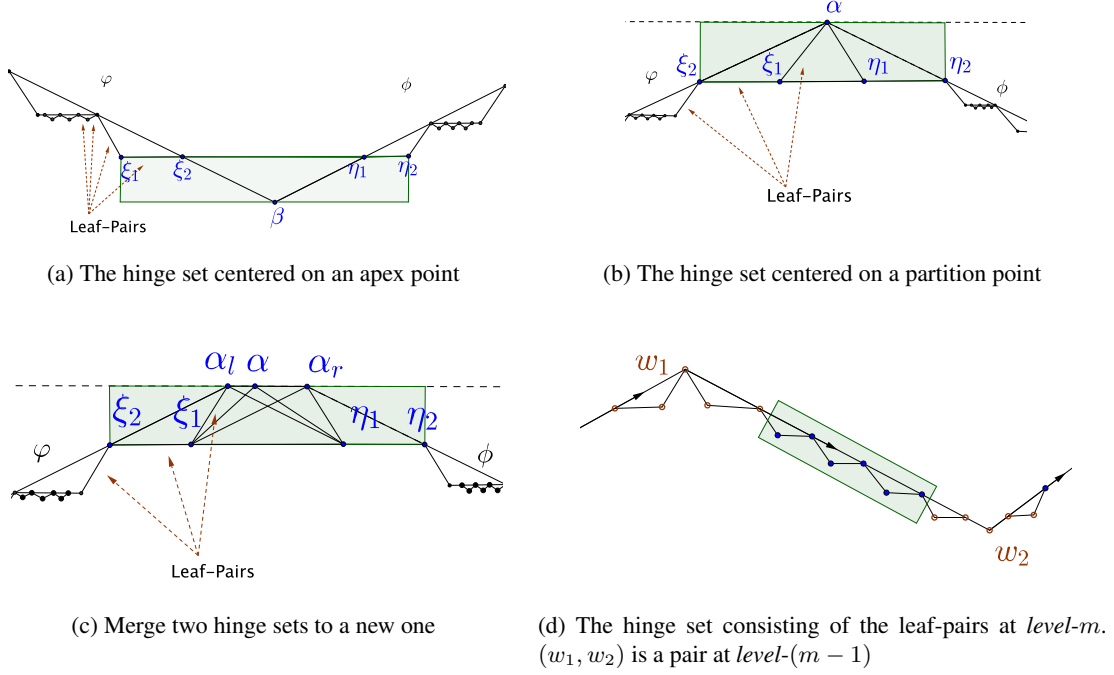


Figure 13: The hinge sets centered on a point in an internal-pair.

- The hinge set centered on a point  $\alpha \in \mathcal{A}_{\hat{\phi}}$ : Suppose  $\alpha$  belongs to one or two internal-pairs in  $\hat{\Phi}$ , which we denote as  $\varphi$  and  $\phi$ .<sup>4</sup> The hinge set centered on  $\alpha$  includes:  $\alpha$  itself, the two child-pairs closest to  $\alpha$  of  $\varphi$  and  $\phi$  respectively (i.e.,  $(\xi_2, \xi_1)$  and  $(\eta_1, \eta_2)$  in Figure 13b). Note that  $\xi_1, \xi_2, \eta_1, \eta_2$  are only incident on leaf-pairs. Besides,  $\alpha$  may be an end point of a short piece and does not belong to any internal-pair in  $\hat{\Phi}$ , i.e.,  $\alpha$  is an isolated point in  $\mathcal{T}$ . Then, for each direction of segment of  $\hat{\phi}$ , we find the closest non-isolated point in  $\mathcal{A}_{\hat{\phi}}$ . Denote them by  $\alpha_l$  and  $\alpha_r$ . Merge the two hinge sets centered on  $\alpha_l$  and  $\alpha_r$  as a new one and add  $\alpha$  in the new hinge set. See Figure 13c.

W.l.o.g, we process the points  $\mu_1$  and  $\mu_2$  in the root pair in the same way as the partition points in  $\mathcal{A}_{(\mu_1, \mu_2)}$ . There are still remaining some points at level- $m$  which do not belong to any hinge set.

- The hinge set consisting of the leaf-pairs at level- $m$ : Consider any pair  $\phi = (w_1, w_2)$  at level- $(m-1)$ . For each set consist of the points which belong to  $\mathcal{A}_{\phi} \cup \mathcal{B}_{\phi}$  but do not belong to the hinge sets of  $w_1$  and  $w_2$ , we define it as a hinge set.<sup>5</sup> See Figure 13d.

Overall, we decompose the points  $\mathcal{P}_m^n$  into a collection of hinge sets. Then, we prove the correctness formally.

**Lemma 14.** *Each point  $p$  in  $\mathcal{P}_m^n$  belongs to exactly one hinge set.*

*Proof.* For convenience, we still use the notations in the construction. First, we prove that any two hinge sets are not overlapping. Consider the first case. If  $\beta$  is one point of an internal-pair,  $\beta$  only belongs the hinge set centered on itself. The two child-pairs of  $\varphi$  incident on  $\xi_1$  are leaf-pairs. Thus, there is no hinge

<sup>4</sup> If  $\alpha$  belongs to only one internal-pair of  $\hat{\Phi}$ , let  $\varphi = \emptyset$ .

<sup>5</sup> Although these points form the leaf-pairs at level- $m$ , these leaf-pairs are the “candidate internal-pairs” to generate the points at level- $(m+1)$ .

set centered on  $\xi_1$ , i.e.,  $\xi_1$  only belongs to the hinge set centered on  $\beta$ . Similarly,  $\xi_2, \eta_1, \eta_2$  only belong to the hinge set centered on  $\beta$ . Then consider the second case.  $\alpha$  is one point of an internal-pair. Thus,  $\alpha$  only belongs to the hinge set centered on itself. Then, any point in  $\{\xi_1, \xi_2, \eta_1, \eta_2\}$  is only incident on leaf-pairs. Thus, there is no hinge set centered on them. They only belong to the hinge set centered on  $\alpha$ . Finally, since any point only has one parent in the tree  $\mathcal{T}$ , the points of the third case only belong to one hinge set. Overall, each point in  $\mathcal{P}_m^n$  belongs to at most one hinge set.

On the other hand, we prove each point in  $\mathcal{P}_m^n$  belongs to at least one hinge set. First, any point of *level- $m$*  belongs to a hinge set according to the third case. Then consider the first two cases. Consider any point of  $\mathcal{A}_{\hat{\phi}}$  and apex point set  $\mathcal{B}_{\hat{\phi}}$ . If it is incident on any internal-pair among the child-pairs of  $\hat{\phi}$ , it should be a center of a hinge set. If the point is an isolated point of  $\mathcal{A}_{\hat{\phi}}$ , it merges two hinge sets and belongs to the new hinge set. The remaining points are the points which are only incident on leaf-pairs of the child-pairs of  $\hat{\phi}$ . Note that for any pair  $\hat{\phi}$  at *level- $t$* ,  $t \leq m - 2$ , only five child-pairs of  $\hat{\phi}$  are leaf-pairs, and only four points of  $\mathcal{A}_{\hat{\phi}} \cup \mathcal{B}_{\hat{\phi}}$  are only incident on leaf-pairs. We have assigned the four points to the two hinge sets centered on the points of  $\hat{\phi}$ .

Overall, each point in  $\mathcal{P}_m^n$  belongs to exactly one hinge set.  $\square$

**Order of the Hinge sets:** Then, we define the total order of all hinge sets. We denote the order by “ $\prec_h$ ”, which is different from the previous order “ $\prec$ ”. The ordering  $\prec_h$  is in fact consistent with the ordering of traversing the fractal path from  $\mu_1$  to  $\mu_2$ . More rigorously, it can be defined as follows.

First, consider the root pair  $(\mu_1, \mu_2)$ . We call the hinge set centered on  $\mu_1$  the *former hinge set* of root, denoted by  $\Lambda_{\mu_1}$ . Call the hinge set centered on  $\mu_2$  the *latter hinge set*, denoted by  $\Lambda_{\mu_2}$ . Define  $\Lambda_{\mu_1}$  as the first hinge set and  $\Lambda_{\mu_2}$  as the last hinge set w.r.t.  $\prec_h$ . Hence  $\Lambda_{\mu_1} \prec_h \Lambda_{\mu_2}$ .

Then we define the orders of other hinge sets. Note that for each internal-pair  $\phi$ , there are two hinge sets centered on the points in  $\phi$ . We call the one closer to (in Euclidean distance) the former hinge set of their parent the *former hinge set* of  $\phi$ , denoted by  $\Lambda_{\phi}^{(-)}$ . Call the other the *latter hinge set* of  $\phi$ , denoted by  $\Lambda_{\phi}^{(+)}$ . Let  $\Lambda_{\phi}^{(-)} \prec_h \Lambda_{\phi}^{(+)}$ . Besides, recall that for any internal-pair  $\phi$  at *level- $(m - 1)$* , the points in  $\mathcal{A}_{\phi} \cup \mathcal{B}_{\phi}$  but not in  $\Lambda_{\phi}^{(-)} \cup \Lambda_{\phi}^{(+)}$  also form a hinge set. We denote it by  $\Lambda_{\phi}$  and define  $\Lambda_{\phi}^{(-)} \prec_h \Lambda_{\phi} \prec_h \Lambda_{\phi}^{(+)}$ .

Note that we have organized all pairs in the recursion tree  $\mathcal{T}$ . We can transform the tree consisting of all **internal nodes** of  $\mathcal{T}$  to a topological equivalent tree  $\mathcal{T}^R$  which has a different ordering of the nodes. The order of the sibling pairs in  $\mathcal{T}^R$  is determined by their Euclidean distances to the former hinge set of their parent. Overall, the ordering  $\prec_h$  of the hinge sets can be defined by a DFS traversing of  $\mathcal{T}^R$ . When we reach a pair  $\phi$  at *level- $t$* ,  $t < m - 1$  in the first time<sup>6</sup>, we visit its former hinge set  $\Lambda_{\phi}^{(-)}$ . Next, we recursively traverse its child-pairs in the order we just defined. Then we return to the pair and visit its latter hinge set  $\Lambda_{\phi}^{(+)}$ . When we reach a pair  $\phi$  at *level- $(m - 1)$* , we visit  $\Lambda_{\phi}^{(-)}, \Lambda_{\phi}, \Lambda_{\phi}^{(+)}$  in order and return.<sup>7</sup>

We claim that only adjacent hinge sets in the above order  $\prec_h$  have edges in the Yao-Yao graph after we introduce some auxiliary points (in Section 5). In order to achieve the purpose, we should break the edges connecting two non-adjacent hinge sets. Formally, we define such edges as the *long range connections* as follows.

**Definition 15** (Long range connection). *We call an edge connecting two points respectively in two non-adjacent hinge sets a long range connection.*

Now, we examine long range connections in  $\text{YY}_{2k+1}(\mathcal{P}_m^n)$ . We show that all long range connections can be organized in a clear way, which is a useful property when we cut the long range connections in Section 5. In order to handle the long range connections conveniently, we give the following claim.

<sup>6</sup>level- $(m - 1)$  is the second to last level of  $\mathcal{T}$  and the last level of  $\mathcal{T}^R$ .

<sup>7</sup>Note that two adjacent sibling pairs share the same hinge set. So the same hinge set may be visited twice, and the two visits are adjacent in the total order. So it does not affect the order between two distinct hinge sets.



---

**Algorithm 3:** TravelHinge( $\phi$ ): Travel the hinge sets in the tree  $\mathcal{T}_\phi^R$

---

```

1 Visit( $\Lambda_\phi^{(-)}$ ) ;
2 if  $\phi$  is at level- $t, t < m - 1$  then
3   foreach child-pair  $\varphi$  of  $\phi$  in  $\mathcal{T}_\phi^R$  do
4     TravelHinge( $\varphi$ ) ;
5 else
6   Visit( $\Lambda_\phi$ )
7 Visit( $\Lambda_\phi^{(+)}$ ) ;

```

---

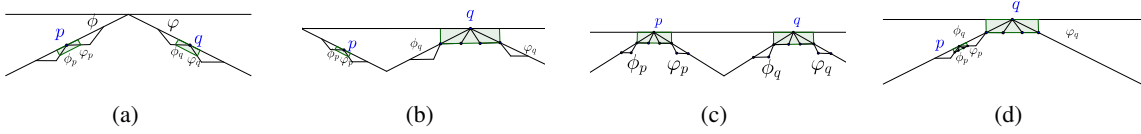


Figure 14: The possible relative positions of  $p$  and  $q$ .

**Claim 16.** Suppose that for any two sibling pairs  $\phi$  and  $\varphi$  at level- $t$  for  $t \leq m - 1$ , there is no long range connection between the points in  $\mathcal{T}_\phi$  and  $\mathcal{T}_\varphi$ . Then, there is no long range connection.

*Proof.* Consider two non-adjacent hinge sets. First, we consider the case that each of them is centered on a point of some internal-pair. Denote the two center points by  $p$  and  $q$  and the two hinge sets by  $\Lambda_p$  and  $\Lambda_q$ .  $p$  belongs to one or two adjacent internal-pairs. W.l.o.g, suppose they are  $\phi_p$  and  $\varphi_p$  ( $\varphi_p = \emptyset$  if  $p$  only belongs to one internal-pair). Meanwhile,  $q$  belongs to one or two adjacent internal-pairs. Suppose they are  $\phi_q$  and  $\varphi_q$ . W.l.o.g, suppose the level of  $\phi_q$  and  $\varphi_q$  is no more than the level of  $\phi_p$  and  $\varphi_p$ . Then, we distinguish two cases. In the first one, none of  $\phi_q$  and  $\varphi_q$  is an ancestor of  $\phi_p$  and  $\varphi_p$ . Otherwise, it is the second case.

Consider the first case. Suppose the closest common ancestor of  $\phi_q, \varphi_q, \phi_p$  and  $\varphi_p$  is  $\hat{\phi}$ . If  $p$  and  $q$  do not belong to  $G_{\hat{\phi}}$ , there are two different child-pairs  $\phi$  and  $\varphi$  of  $\hat{\phi}$  (see Figure 14a), such that  $\Lambda_p$  belongs to  $\mathcal{T}_\phi$  and  $\Lambda_q$  belongs to  $\mathcal{T}_\varphi$ . Since points between  $\mathcal{T}_\phi$  and  $\mathcal{T}_\varphi$  have no long range connection according to the assumption, points between  $\Lambda_p$  and  $\Lambda_q$  have no long range connection. Then consider  $q$  belongs to  $G_{\hat{\phi}}$  (see Figure 14b). Note that  $\Lambda_q$  is a subset of  $\mathcal{T}_{\phi_q} \cup \mathcal{T}_{\varphi_q}$ . Because there is no long range connections for the points between  $\mathcal{T}_{\phi_q}, \mathcal{T}_{\varphi_q}$  and  $\mathcal{T}_\varphi$ ,  $\Lambda_p$  and  $\Lambda_q$  have no long range connection. Finally, if both  $p$  and  $q$  belong to  $G_{\hat{\phi}}$  (see Figure 14c), since there is no long range connections for points between  $\mathcal{T}_{\phi_p}, \mathcal{T}_{\varphi_p}$  and  $\mathcal{T}_{\phi_q}, \mathcal{T}_{\varphi_q}$ ,  $\Lambda_p$  and  $\Lambda_q$  have no long range connection.

Consider the second case. See Figure 14d. W.l.o.g., suppose  $\phi_p$  and  $\varphi_p$  are in the subtree of  $\mathcal{T}_{\phi_q}$ .  $\Lambda_q$  is a subset of  $\mathcal{T}_{\phi_q} \cup \mathcal{T}_{\varphi_q}$ . Moreover, the points between  $\mathcal{T}_{\phi_q}$  and  $\mathcal{T}_{\varphi_q}$  have no long range connections. Since  $\phi_p$  and  $\varphi_p$  are in the subtree of  $\mathcal{T}_{\phi_q}$ , we know that the points in  $\Lambda_q \cap \mathcal{T}_{\varphi_q}$  have no long range connections to  $\Lambda_p$ . Then we consider the long range connection between  $\Lambda_q \cap \mathcal{T}_{\phi_q}$  and  $\Lambda_p$ . Actually, it is the first case, thus they have no long range connection.

Now, we have discussed the case that each of the two hinge sets is centered on a point of some internal-pair. Then suppose that at least one of the hinge sets contains only leaf-pairs at level- $m$ , i.e., is a third type hinge set. If both of them are the third type hinge sets, denoted by  $\Lambda_\phi$  and  $\Lambda_\varphi$ , there must exist two sibling pairs  $\hat{\phi}$  and  $\hat{\varphi}$  such that  $\Lambda_\phi \in \mathcal{T}_{\hat{\phi}}$  and  $\Lambda_\varphi \in \mathcal{T}_{\hat{\varphi}}$ . According to the hypothesis of the lemma, there is no long range connection between  $\Lambda_\phi$  and  $\Lambda_\varphi$ . Finally, consider the case that there is only one third type hinge set, denoted by  $\Lambda_\phi$  and the other is centered on  $q$ , denoted by  $\Lambda_q$ . Suppose  $q$  is the shared point of  $\varphi_q$  and  $\phi_q$ .

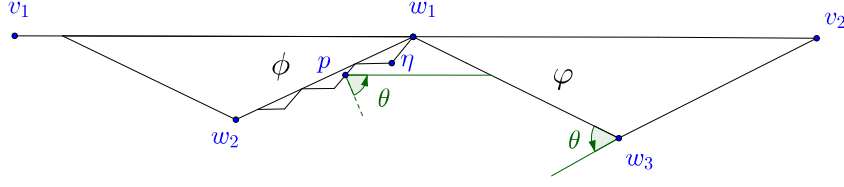


Figure 15: The edge  $pw_3$  cannot be accepted in the reverse-Yao step. Because  $\eta w_3$  exists in the Yao-step. Besides,  $\eta$  and  $p$  are in the same cone of  $w_3$  and  $|\eta w_3| < |pw_3|$ . Thus,  $pw_3$  is rejected in the reverse-Yao step. Note that  $\eta w_3$  is a hinge connection.

We distinguish two cases according to whether  $\phi \in \mathcal{T}_{\phi_q} \cup \mathcal{T}_{\varphi_q}$  or not. As we discuss above, we can prove that there is no long range connection between  $\Lambda_q$  and  $\Lambda_\phi$ .  $\square$

Then we discuss the possible long range connections between  $\mathcal{T}_\phi$  and  $\mathcal{T}_\varphi$  for two sibling pairs  $\phi$  and  $\varphi$ .  $p$  belongs to  $\mathcal{T}_\phi$  and  $q$  belongs to  $\mathcal{T}_\varphi$ . In the following, we prove that if the directed edge  $\vec{pq}$  is an edge in  $\text{YY}_{2k+1}(\mathcal{P}_m^n)$ , then  $\phi \prec \varphi$ . Moreover, note that the points of  $\mathcal{T}_\varphi$  locate in at most two cones of  $p$ . We prove that for each point  $p$ , only one of the two cones may contain a long range connection. First, we prove the observation as follows.

**Observation 17.** *Consider two sibling pairs  $\phi$  and  $\varphi$  such that  $\phi \prec \varphi$ . Suppose  $p$  belongs to  $\mathcal{T}_\phi$ . If  $\varphi$  is a leaf-pair, there is no long range connection between  $p$  and the points of  $\varphi$ .*

*Proof.* See Figure 15 for an illustration. W.l.o.g, suppose  $\phi = (w_1, w_2)$  and  $\varphi = (w_3, w_1)$ . It is not difficult to check that there is no edge between  $p$  and  $w_1$  in the Yao-step. Let  $\eta$  be the point in  $G_\phi$  closest to  $w_1$ . If directed edge  $pw_2$  is accepted in the Yao-step,  $pw_2$  cannot be accepted in the reverse-Yao step since  $\eta w_3$  exists in the Yao-step, and  $\eta$  and  $p$  are in the same cone of  $w_3$  and  $|\eta w_3| < |pw_3|$ . Note that  $\eta w_3$  is a hinge connection. Thus, there is no long range connection between  $\phi$  and  $\varphi$ .  $\square$

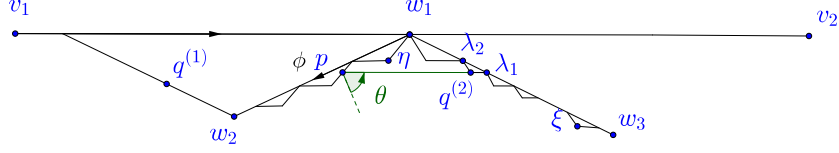
Given a pair  $(v_1, v_2)$  with child-pair set  $\Phi$ , consider two sibling pairs  $\phi$  and  $\varphi$  in  $\Phi$  where  $\phi = (w_1, w_2)$ . For convenience, let  $\angle u_1 u_2$  be the polar angle of vector  $u_1 u_2$ . Let  $\angle(u_1 u_2, v_1 v_2)$  be  $\angle v_1 v_2 - \angle u_1 u_2$ , i.e., the angle from  $u_1 u_2$  to  $v_1 v_2$  in the anticlockwise direction.

Recall that there are two kinds of normal points according to the definition of gadget: partition points and apex points. According to the type of point  $w_1$  and the relative position between  $\phi = (w_1, w_2)$  and  $(v_1, v_2)$ , there are four cases: (1)  $w_1$  is a partition point and  $\phi$  is on the right side of  $v_1 v_2$ , (2)  $w_1$  is an apex point and  $\phi$  is on the left side of  $v_1 v_2$ , (3)  $w_1$  is a partition point and  $\phi$  is on the left side of  $v_1 v_2$ , (4)  $w_1$  is an apex point and  $\phi$  is on the right side of  $v_1 v_2$ . See Figure 16 and 18 for illustrations.

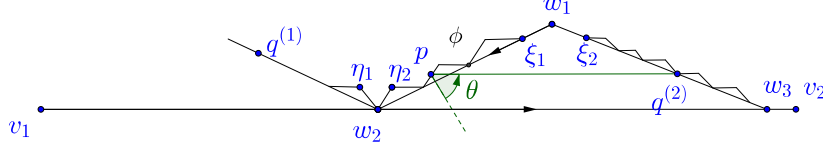
Then we prove the possible long range connections between the points of  $\mathcal{T}_\phi$  and  $\mathcal{T}_\varphi$  case by case. Lemma 18 covers case (1) and case (2) which satisfy the condition  $\angle(v_1 v_2, w_2 w_1) = \theta/2$ . Lemma 19 covers case (3) and case (4) which satisfy the condition  $\angle(v_1 v_2, w_2 w_1) = -\theta/2$ .

**Lemma 18.** *Given a pair  $(v_1, v_2)$  with child-pair set  $\Phi$ , consider two sibling pairs  $\phi$  and  $\varphi$  in  $\Phi$  where  $\phi = (w_1, w_2)$ .  $\phi$  and  $\varphi$  are at level- $t$  for  $t \leq m - 1$ . Suppose point  $p$  belongs to  $\mathcal{T}_\phi$  and  $q$  belongs to  $\mathcal{T}_\varphi$ . If  $\angle(v_1 v_2, w_2 w_1) = \theta/2$  and there is a directed edge from  $p$  to  $q$  in  $\text{YY}_{2k+1}(\mathcal{P}_m^n)$ , then  $\angle(v_1 v_2, pq) = 0$  (i.e.,  $pq$  is parallel to  $v_1 v_2$ ), and  $q$  is a point in the gadget  $G_\varphi$  generated by  $\varphi$ .*

*Proof.* As we discuss above, there are two cases under the conditions. Consider case (1). See Figure 16a. First, we prove that  $\angle(v_1 v_2, pq)$  should belong to  $(-\theta/2, 0]$ . If  $q$  belongs to  $\mathcal{T}_\varphi$  and  $\varphi \prec \phi$  (i.e.,  $q = q^{(1)}$  in Figure 16a),  $w_2$  and  $q$  are in the same cone of  $p$ . There is no edge from  $p$  to  $q$  since  $|pw_2| < |pq|$  and the edge  $pq$  is rejected in the Yao-step. Then consider that  $q$  belongs to  $\mathcal{T}_\varphi$  and  $\varphi \succ \phi$  (i.e.,  $q = q^{(2)}$  in

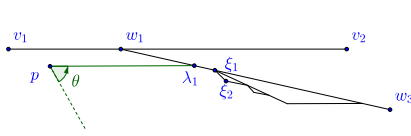


(a) Case 1:  $w_1$  is the partition point and  $\phi$  is on the right side of  $v_1v_2$

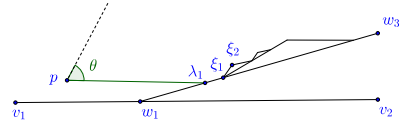


(b) Case 2:  $w_1$  is the apex point and  $\phi$  is on the left side of  $v_1v_2$

Figure 16: The two cases about  $\angle(v_1v_2, w_2w_1) = \theta/2$ . Here  $\phi = (w_1, w_2)$  and  $p \in \mathcal{T}_\phi$ .



(a) The degenerated case for case 1 in Lemma 18



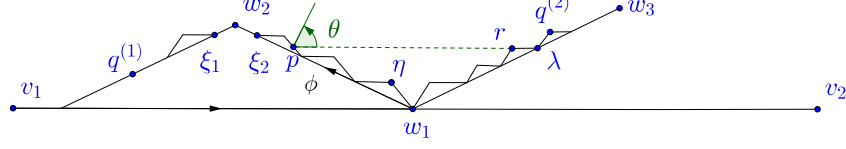
(b) The degenerated case for case 3 in Lemma 19

Figure 17: The degenerated cases in which the projection point of  $p$  is an isolated partition point, i.e.,  $\lambda_1$  in the figure is an isolated partition point which is incident on a short piece.

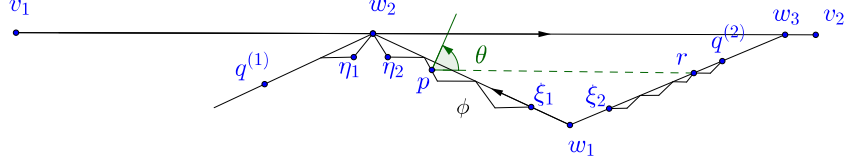
Figure 16a). According to Observation 17, we safely assume that  $\varphi$  is an internal-pair. Denote the point in  $G_\phi$  closest to  $w_1$  by  $\eta$ . If  $\angle(v_1v_2, pq) > 0$ ,  $\eta$  and  $q$  are in the same cone of  $p$  since  $w_1\eta$  has the maximum length among its sibling pairs according to Corollary 12. Thus, there is no edge from  $p$  to  $q$  in the Yao-step since  $|p\eta| < |pq|$ . Thus,  $\angle(v_1v_2, pq) \in (-\theta/2, 0]$ . Then, we prove that  $\angle(v_1v_2, pq) = 0$ . Suppose the projection point of  $p$  to pair  $\varphi$  is  $\lambda_1$  (the  $\lambda_1$  must exist according to the process projection) and  $q$  is an apex point of the piece  $\lambda_1\lambda_2$ . Note that  $\theta < \pi/3$  for  $k \geq 3$  and the maximum length among child-pairs of  $\varphi$  is at most twice longer the minimum one (according to the refinement). It is not difficult to check the point closest to  $p$  in cone  $C_p(-\theta, 0]$  is  $q$ . Thus,  $pq$  is parallel to  $v_1v_2$ .

Note that there is a degenerated case in which the projection  $\lambda_1$  is an end point of an empty piece. Thus, we do not generate the corresponding apex point  $q$ . See Figure 17a for an illustration.  $(\xi_2, \xi_1)$  is the pair closest to  $\lambda_1$ . Note that for  $k \geq 3$ , the angle  $\angle p\lambda_1\xi_2 > \pi/2$  and  $(\xi_1, \xi_2)$  is a leaf. Thus, in this degenerated case, the point closest to  $p$  in cone  $C_p(-\theta, 0]$  is  $\lambda_1$ .  $p\lambda_1$  is also parallel to  $v_1v_2$ . Thus, the lemma is still true. We can process the degenerated case in the same framework in the following and do not distinguish the degenerated case particularly.

Consider case (2). See Figure 16b. Suppose  $\eta_2$  is the apex point of the near-empty piece of  $\phi$  incident on  $w_2$ . Note that  $w_2\eta_2$  has the maximum length among its sibling pairs. If  $q$  belongs to  $\mathcal{T}_\varphi$  and  $\varphi \prec \phi$  (i.e.,  $q = q^{(1)}$  in Figure 16b),  $\eta_2$  and  $q$  are in the same cone of  $p$  and  $|\eta_2p| < |qp|$ . Thus, there is no edge from  $p$  to  $q$  in the Yao-step. Then consider that  $q$  belongs to  $\mathcal{T}_\varphi$  and  $\varphi \succ \phi$  (i.e.,  $q = q^{(2)}$  in Figure 16b). According to Observation 17, we assume that  $\varphi$  is an internal-pair. If  $\varphi \succ \phi$ , the polar angle of  $pq$  should belong to  $(-\theta/2, 0]$ . If not,  $w_1$  and  $q$  are in the same cone. Thus, there is no edge from  $p$  to  $q$  in the Yao-step since



(a) Case 3:  $w_1$  is the partition point and  $\phi$  is on the left side of  $v_1v_2$



(b) Case 4:  $w_1$  is the apex point and  $\phi$  is on the right side of  $v_1v_2$

Figure 18: The two cases about  $\angle(v_1v_2, w_2w_1) = -\theta/2$ . Here  $\phi = (w_1, w_2)$  and  $p \in \mathcal{T}_\phi$ .

$|pq| > |pw_1|$ . Then we prove that  $pq$  is parallel to  $v_1v_2$ . The point closest to  $p$  in the cone  $C_p(-\theta, 0]$  is the projection point of  $p$  ( $p$  must exist because of the projection). Thus,  $pq$  is parallel to  $v_1v_2$ .  $\square$

**Lemma 19.** *Given a pair  $(v_1, v_2)$  with child-pair set  $\Phi$ , consider two sibling pairs  $\phi$  and  $\varphi$  in  $\Phi$  where  $\phi = (w_1, w_2)$ . Suppose  $\phi$  and  $\varphi$  are at level- $t$  for  $t \leq m - 1$ . Suppose point  $p$  belongs to  $\mathcal{T}_\phi$ , and  $q$  belongs to  $\mathcal{T}_\varphi$ . If  $\angle(v_1v_2, w_2w_1) = -\theta/2$  and there is a directed edge from  $p$  to  $q$  in  $\mathbb{Y}\mathbb{Y}_{2k+1}(\mathcal{P}_m^n)$ , then  $\angle(v_1v_2, pq) \in (0, \theta/2)$ . Moreover, there exists a point  $r$  in  $\mathcal{T}_\varphi$  such that  $pr$  is parallel to  $v_1v_2$  and  $|pr| < |pq|$ . Moreover,  $r$  is a point in the gadget  $G_\varphi$  generated by  $\varphi$ .*

*Proof.* As we discuss above, case (3) and (4) satisfy the condition  $\angle(v_1v_2, w_2w_1) = -\theta/2$ . Suppose  $q$  belongs to  $\mathcal{T}_\varphi$ . Consider case (3). See Figure 18a. Suppose  $w_2\xi_1$  and  $w_2\xi_2$  are the two empty pieces incident on  $w_2$ . If  $q$  is in  $\mathcal{T}_\varphi$  and  $\varphi \prec \phi$  (i.e.,  $q = q^{(1)}$  in Figure 18a),  $\xi_1$  and  $q$  are in the same cone of  $p$ . If  $q$  is not  $\xi_1$ , there is no edge from  $p$  to  $q$  even in the Yao-step since  $|p\xi_1| < |pq|$ . If  $q$  is  $\xi_1$ ,  $p\xi_1$  would not be accepted by  $\xi_1$  in the reverse-Yao step, since there is an edge from  $\xi_2$  to  $\xi_1$  and  $|\xi_1\xi_2| < |p\xi_1|$ . Then consider that  $q$  (i.e.,  $q = q^{(2)}$  in Figure 18a) is in  $\mathcal{T}_\varphi$  and  $\varphi \succ \phi$ . According to Observation 17, we safely assume that  $\varphi$  is an internal-pair. Thus,  $\angle(v_1v_2, pq) \in [-\theta/2, \theta/2)$ . If  $\angle(v_1v_2, pq) \in [-\theta/2, 0]$ ,  $pq$  is not a directed edge in Yao-step since  $w_1$  and  $q$  are in the same cone and  $|w_1p| < |pq|$ . Finally, consider the projection point  $\lambda$  ( $\lambda$  exists because of the projection) of  $p$  to pair  $\varphi$ .  $r$  is the apex point related to  $\lambda$  and on the segment  $p\lambda$ . It is not difficult to check that  $|pr| < |pq|$  since  $\theta/2 \leq \pi/2$  and the maximum length among the non-empty pieces of  $\varphi$  is at most twice longer the minimum one (according to refinement). Similar to case 1 in Lemma 18, there is a degenerated case that  $\lambda$  is the end point of an empty piece. See Figure 17b. In this case, it is not difficult to check  $|p\lambda| < |pq|$ .

Consider case (4). See Figure 18b. Suppose  $\eta_1$  and  $\eta_2$  are the apex points of the near-empty pieces incident on  $w_2$ . If  $q$  is in  $\mathcal{T}_\varphi$  and  $\varphi \prec \phi$  (i.e.,  $q = q^{(1)}$  in Figure 18b),  $\eta_1$  and  $q$  are in the same cone of  $p$ . If  $q$  is not  $\eta_1$ , there is no edge from  $p$  to  $q$  in the Yao-step since  $|p\eta_1| < |pq|$ . If  $q$  is  $\eta_1$ ,  $p\eta_1$  would not be accepted by  $\eta_1$  in the reverse-Yao step since there is an edge from  $\eta_2$  to  $\eta_1$  and  $|\eta_1\eta_2| < |p\eta_1|$ . Then consider  $q$  is in  $\mathcal{T}_\varphi$  and  $\varphi \succ \phi$  (i.e.  $q = q^{(2)}$  in Figure 18b). Based on Observation 17, we assume that  $\varphi$  is an internal-pair. The polar angle of  $pq$  should belong to  $(0, \theta/2)$ . If not,  $w_1$  and  $q$  are in the same cone. Thus, there is no edge from  $p$  to  $q$  since  $|pq| > |pw_1|$ . Finally, consider the projection point  $r$  of  $p$  ( $r$  must exist because of the projection) to pair  $\varphi$ .  $|pr| < |pq|$  and  $pr$  is parallel to  $v_1v_2$  since  $\theta/2 \leq \pi/2$ .  $\square$

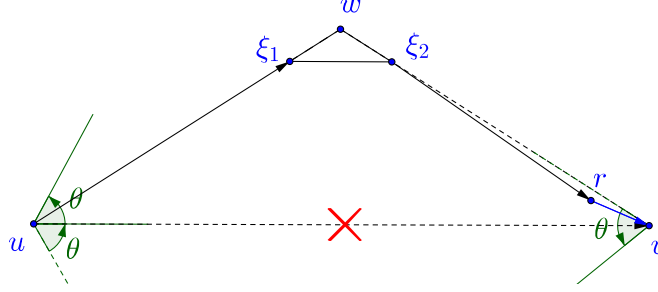


Figure 19: A simple example to explain how an auxiliary point cutting a long range connection.

In the next section, we discuss how to cut such long range connections. Roughly speaking, under the condition of Lemma 18, we can cut the long range connection  $pq$  through adding two auxiliary points close to  $q$ . Under the condition of Lemma 19, we can cut the long range connection  $pq$  through adding two auxiliary points close to  $r$ .

Based on Lemma 18 and 19, we have the corollary as follows.

**Corollary 20.** *Consider two sibling pairs  $\phi$  and  $\varphi$  with subtrees  $\mathcal{T}_\phi$  and  $\mathcal{T}_\varphi$  respectively. Suppose  $p$  belongs to  $\mathcal{T}_\phi$  and  $q$  belongs to  $\mathcal{T}_\varphi$ . If directed edge  $\vec{pq}$  is in  $\text{YY}_{2k+1}(\mathcal{P}_m^n)$ , then  $\phi \prec \varphi$ .*

## 5 The Positions of Auxiliary Points

Then, we discuss how to use the auxiliary points to cut the long range connections in the Yao-Yao graph  $\text{YY}_{2k+1}(\mathcal{P}_m^n)$ . Denote the set of auxiliary points by  $\mathcal{P}_m^a$ . Let  $\mathcal{P}_m = \mathcal{P}_m^n \cup \mathcal{P}_m^a$ .

First, we consider a simple example to see how auxiliary points work. Consider three points  $u, v$  and  $w$ .  $uv$  is horizontal, and  $\angle wvu = \angle wuv = \theta/2$ . The point  $\xi_1$  and  $\xi_2$  are two points on segment  $uw$  and  $vw$  respectively.  $\xi_1\xi_2$  is horizontal. See Figure 19. Note that the polar angles of a cone in the Yao-Yao graph belong to a half-open interval in the anticlockwise direction. Thus,  $uv$  is in the  $\text{YY}_{2k+1}$  graph, which is the shortest path between  $u$  and  $v$ . However, we can add an auxiliary point  $r$  close to  $v$  and  $\angle rvu < \theta/2$ . Then according to the definition of Yao-Yao graphs, the point  $v$  rejects the edge  $uv$  in the reverse-Yao step since  $rv$  exists in the Yao-step, and point  $r$  and  $u$  are in the same cone of  $v$  and  $|rv| < |vu|$ . Moreover,  $ur$  and  $r\xi_1$  are not edges in the Yao-Yao graph. Note that directed edge  $ur$  is not in Yao graph since  $\xi_1$  and  $u$  are in the same cone of  $r$  and  $|\xi_1u| < |ur|$ . The directed edge  $ru$  is not in Yao graph since  $\xi_1$  and  $u$  are in the same cone of  $r$  and  $|\xi_1r| < |ur|$ . Besides, directed edge  $\xi_1r$  is not in the Yao graph since  $r$  and  $\xi_2$  are in the same cone of  $\xi_1$  and  $|\xi_1\xi_2| < |\xi_1r|$ . Finally, directed edge  $r\xi_1$  is not accepted by  $\xi_1$  in the reverse-Yao step since there is an edge  $\xi_2\xi_1$  in the same cone of  $r$  and  $|\xi_2\xi_1| < |r\xi_1|$ . Overall, the shortest path between  $uv$  becomes  $u\xi_1\xi_2rv$ .

**The positions of the auxiliary points:** Now, we explain the positions of the auxiliary points formally. We call the normal point closest to an auxiliary point the *center* of the auxiliary point. Then, we use the polar coordinate to describe the relative location of an auxiliary point to its center.

For convenience, we define some parameters first. Let  $\Delta$  be the minimum distance between any two normal points and  $n$  be the number of the normal points. Recall that we partition the root pair  $\mu_1, \mu_2$  into  $d_0$  equidistant pieces. Let  $\gamma$  be a very small angle, such as  $\gamma = \theta d_0^{-1}$ . Let  $\sigma = \max\{\sin(\theta/2 - \gamma)/\sin \gamma, \sin^{-1}(\theta/2 - \gamma)\} + \epsilon$  for some small  $\epsilon > 0$ . Let  $\chi = d_0 \sigma^n \Delta^{-1}$ . Roughly speaking,  $\chi \gg d_0 > \sigma > 1$ .

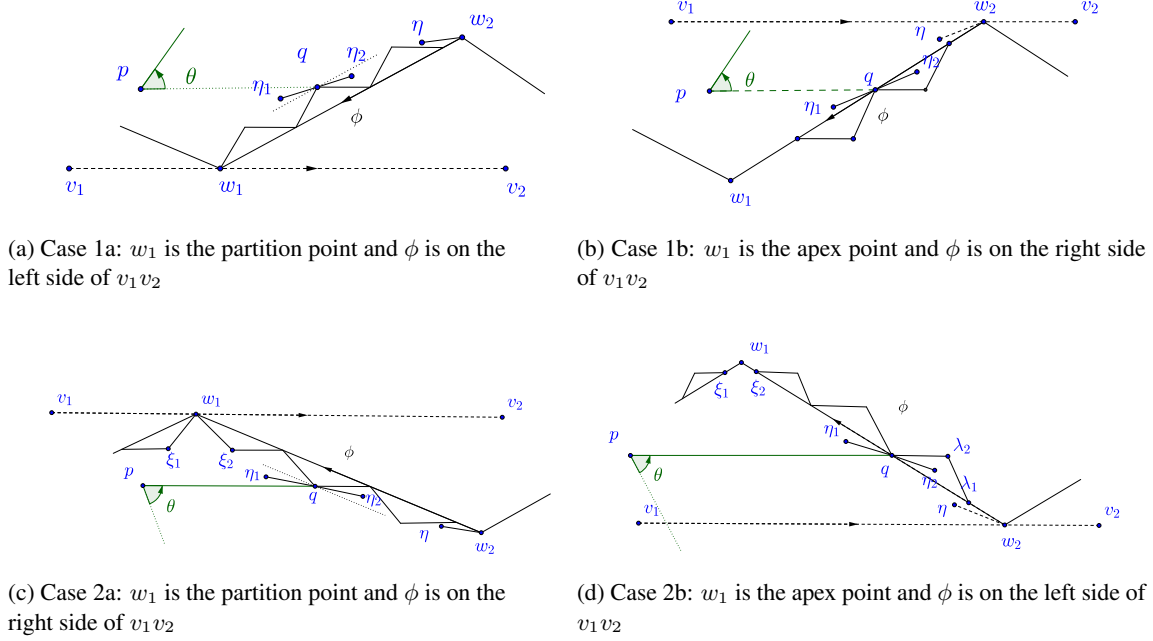


Figure 20: The auxiliary points for each point. Here  $\phi = (w_2, w_1)$  and  $q \in \mathcal{G}_\phi$ .  $\eta_1$  and  $\eta_2$  are two auxiliary points centered on  $q$ . Note that  $|\eta_1 q|$  and  $|\eta_2 q|$  are very small in fact. This is just a diagram to explain the relative positions between  $\{\eta_1, \eta_2\}$  and  $q$ .

**Definition 21** (Candidate center). *Consider a pair  $(v_1, v_2)$  and a set  $\Phi$  of its child-pairs. Suppose  $\phi, \varphi \in \Phi$  and  $\varphi \prec \phi$ .  $p$  is a point in  $\mathcal{T}_\varphi$ . Suppose one projection point of  $p$  is in  $\mathcal{T}_\phi$ . Thus, there exists a point  $q$  closest to  $p$  such that  $q \in \mathcal{T}_\phi$  and  $pq$  is parallel to  $v_1v_2$ . We call such a point  $q$  a candidate center of auxiliary points.*

According to Lemma 18 and 19, each candidate center  $q$  in  $\mathcal{T}_\phi$  is a point in gadget  $\mathcal{G}_\phi$ . We will prove in Lemma 24 that we can add some auxiliary points centered on  $q$  such that there is no long range connection from  $p$  to  $\mathcal{T}_\phi$  and the auxiliary points do not introduce new long range connections.

Then, we explain the process to add auxiliary points centered on  $q$ . Note that if there is a point  $p \in \mathcal{T}_\varphi$  which has a projection point in  $\mathcal{T}_\phi$ , then  $\varphi \prec \phi$  according to our construction. Thus, we can add auxiliary points in the DFS preorder of  $\phi$  w.r.t. to  $\mathcal{T}$ . It means that we traverse  $\mathcal{T}$  in the DFS preorder. Each time we reach a pair  $\phi$ , we find all candidate centers in  $\mathcal{G}_\phi$  and add auxiliary points centered on them. Moreover, let the order of  $\phi$  in the DFS preorder w.r.t. to  $\mathcal{T}$  be  $\kappa$ . The distance between the auxiliary point and  $q$  depends on  $\kappa$ .<sup>8</sup> After processing all points  $q$ , combining with Lemma 18 and 19 and Claim 16, there is no long range connections in  $\mathcal{P}_m$ .

Let  $\phi = (w_2, w_1)$ . There are two cases according to  $\angle(v_1v_2, w_1w_2) = \theta/2$  or  $-\theta/2$ .

- $\angle(v_1v_2, w_1w_2) = \theta/2$  (see Figure 20a and 20b): We add two points  $\eta_1$  and  $\eta_2$  centered on  $q$  such that  $\angle(w_2w_1, q\eta_1) = \angle(w_2w_1, q\eta_2) = -\gamma$  and  $|q\eta_1| = |q\eta_2| = \sigma^\kappa \chi^{-1}$ , except when  $q = w_2$ . If  $q = w_2$ , we only add the point  $\eta_1$  (see Figure 20a and 20b, where  $\eta_1 = \eta$ ).
- $\angle(v_1v_2, w_1w_2) = -\theta/2$  (see Figure 20c and 20d): We add two points  $\eta_1$  and  $\eta_2$  centered on  $q$  such that  $\angle(w_2w_1, q\eta_1) = \angle(w_2w_1, q\eta_2) = \gamma$  and  $|q\eta_1| = |q\eta_2| = \sigma^\kappa \chi^{-1}$ , except when  $q = w_2$  or

<sup>8</sup>Note that  $\kappa$  is the order of  $\phi$ , not the order of a pair containing  $q$ . Since each point may belong to two pairs but only has one parent-pair.



$p$  and  $q$  are in the same hinge set. If  $q = w_2$  we only add the point  $\eta_1$  (see Figure 20c and 20d, where  $\eta_1 = \eta$ ). Moreover, if  $p$  and  $q$  are in the same hinge set (i.e., the points  $\xi_1, \xi_2$  in Figure 20c or 20d), we add two points  $\eta_1$  and  $\eta_2$  centered on  $q$  such that  $\angle(w_2 w_1, q\eta_1) = \angle(w_2 w_1, \eta_2 q) = \gamma$  and  $|q\eta_1| = |\eta_2 q| = \sigma^\kappa \chi^{-1} + \epsilon_0$  where  $\epsilon_0$  is much less than the distance between any two points in  $\mathcal{P}_m$ .<sup>9</sup>

First, we list some obvious properties of the auxiliary points as follows.

**Property 22.** *P1 The maximum length between an auxiliary point and its center is at most  $d_0^{-1} \Delta$ .*

*P2 Any point  $q \in \mathcal{P}_m^n$  can become a candidate center of auxiliary points at most twice.*

*P3 There are at most three auxiliary points centered on a normal point.*

*P4 Suppose  $q$  is a candidate center because of the projection of  $p$ . Thereby we add the auxiliary point  $\eta$  centered on  $q$ . If there is an auxiliary point  $\xi$  centered on  $p$ , then  $|\xi p| \leq \sigma^{-1} |\eta q|$ . Hence, the perpendicular distance from  $\eta$  to the line  $pq$  is larger than  $|\xi p|$ .*

*P5 If auxiliary points  $\eta_1, \eta_2$  and  $\eta_3$  are centered on  $q$  and  $|q\eta_1| = |q\eta_2|$ , then  $|q\eta_1| \leq \sigma^{-1} |q\eta_3|$ ,  $\angle\eta_2 q \eta_3 = (\theta/2 - 2\gamma)$ , and  $\angle q \eta_3 \eta_2 < \gamma$ .*

*Proof.* In the proof, we use the same notations as in the construction and prove the properties in turns as follows.

[P1] Note that the largest  $\kappa$  is at most  $n$  since there are at most  $n$  pairs in the tree. The maximum length between the auxiliary point and its center is at most  $\sigma^n \chi^{-1} = d_0^{-1} \Delta$ .

[P2] Note that each point  $q \in \mathcal{P}_m^n$  belongs to at most three gadgets. Denote the parent-pair of these gadgets by  $\phi_1, \phi_2, \phi_3$ . W.l.o.g, suppose  $\phi_2$  and  $\phi_3$  are the child-pairs of  $\phi_1$ . Thus,  $q \in \mathcal{A}_{\phi_1}$  and  $q \in \phi_2 \cap \phi_3$ . Denote  $\phi_2 \prec \phi_3$ . We visit  $\phi_1$  first and  $\phi_2$  and  $\phi_3$  in order. Note that  $q$  is the shared point of  $\phi_2$  and  $\phi_3$ . It means that when we visit  $\phi_3$ ,  $q$  cannot be a candidate center. Hence, there are only two times that  $q$  can become a candidate center. The first time happens when we visit  $\phi_1$  and the second time happens when we visit  $\phi_2$ .

[P3] Followed by the proof of [P2], in the first time, we add two auxiliary points centered on  $q$ . In the second time, we add one auxiliary point centered on  $q$ . Thus, there are at most three auxiliary points centered on a normal point.

[P4] Suppose  $p$  belongs to subtree  $\mathcal{T}_\varphi$  and  $q$  belongs to subtree  $\mathcal{T}_\phi$  and  $\varphi \prec \phi$ . Thus, the auxiliary points are added for  $p$  earlier than  $q$ . It means that  $|\xi p| \leq \sigma^{-1} |\eta q|$ . Note that the acute angle between  $\eta q$  and  $pq$  is  $(\theta/2 - \gamma)$  and  $\sigma > \sin^{-1}(\theta/2 - \gamma)$ . Thus, the perpendicular distance from  $\eta$  to the line  $pq$  is larger than  $|\xi p|$ . See Figure 21.

[P5] According to the proof of [P3], we add  $\eta_1$  and  $\eta_2$  earlier than  $\eta_3$ . According to the construction, we can add the three auxiliary points for  $q$ . Checking the four cases in construction, we can get  $\angle(pq, q\eta_3) = -\gamma$  and  $\angle(pq, q\eta_2) = -\theta/2 + \gamma$ . Thus,  $\angle\eta_2 q \eta_3 = \theta/2 - 2\gamma$ . Moreover, note that  $\sigma > \sin(\theta/2 - \gamma)/\sin \gamma$  and  $|\eta_2 q| < \sigma^{-1} |\eta_3 q|$ . According to the law of sines, we get  $\angle q \eta_3 \eta_2 < \gamma$ . See Figure 22.  $\square$

**Extended hinge set:** We generalize the concept of hinge sets to the *extended hinge set* to include auxiliary points. The extended hinge set consists of the normal points in the hinge set and the auxiliary points centered on these normal points. Besides, if  $p$  belongs to  $\mathcal{T}_\phi$ , we say the auxiliary points centered on  $p$  also belonging to *extended*  $\mathcal{T}_\phi$ . Then Claim 16 is still true for  $\text{YY}_{2k+1}(\mathcal{P}_m)$  with the same proof. It means that we only need to consider the long range connections between the descendants of any two sibling pairs.

<sup>9</sup> It is slightly different from the first case as above. We add two auxiliary points with distance slightly larger than  $\sigma^\kappa \chi^{-1}$  to its center when  $p$  and  $q$  are in the same hinge set. The reason is that the cone is half-open half-close in the anticlockwise direction. It will help a lot to unify the proof in the same framework. See details in the proof of Lemma 23.



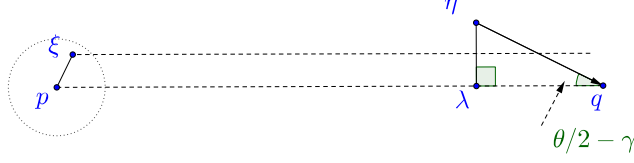


Figure 21:  $|\xi p| \leq \sigma^{-1}|\eta q|$  for the auxiliary point of  $p$ . Moreover, the perpendicular distance from  $\eta$  to  $pq$  (i.e.,  $|\eta\lambda|$  in the figure) is larger than  $|\xi p|$ .

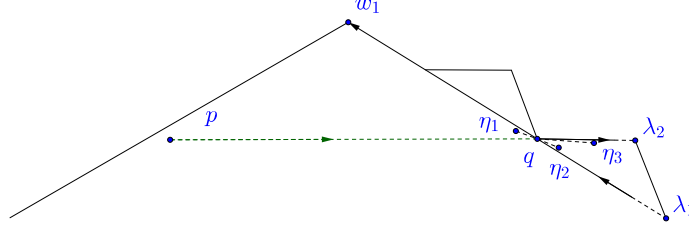


Figure 22: The relative positions of the three auxiliary points of a partition point  $q$ .

Moreover, we can get similar properties as Lemma 18 and 19 for the auxiliary points. Suppose  $\phi$  and  $\varphi$  are two sibling pairs. If  $p \in \mathcal{T}_\phi$  and  $q \in \mathcal{T}_\varphi$  and there is a long range connection  $\vec{pq}$  in  $\mathbb{Y}\mathbb{Y}_{2k+1}$ , then  $\phi \prec \varphi$ . Meanwhile, the points in  $\mathcal{T}_\varphi$  locate in two cones of  $p$ . But only one of the two cones may exist a long range connection. We describe the lemma in a more compact way as follows.

**Lemma 23.** *Given a pair  $(v_1, v_2)$  at level- $t$  for  $t < m - 1$ , with child-pair set  $\Phi$ , consider two sibling pairs  $\phi$  and  $\varphi$  in  $\Phi$  where  $\phi = (w_1, w_2)$ .  $p$  is a point in extended  $\mathcal{T}_\phi$  and  $q$  is a point in extended  $\mathcal{T}_\varphi$ . Suppose there is a directed edge  $pq$  in  $\mathbb{Y}\mathbb{Y}_{2k+1}(\mathcal{P}_m)$ .*

- If  $\angle(v_1v_2, w_2w_1) = \theta/2$ , then  $\angle(v_1v_2, pq) \in (-\theta, 0]$ .
- If  $\angle(v_1v_2, w_2w_1) = -\theta/2$ , then  $\angle(v_1v_2, pq) \in (0, \theta]$ .

*Proof.* The proof is almost the same as that of Lemma 18 and 19. We can also distinguish into two cases. Given a pair  $(v_1, v_2)$  and its child-pair set  $\Phi$ , consider two sibling pairs  $\phi$  and  $\varphi$  in  $\Phi$  where  $\phi = (w_1, w_2)$ . The first case is that  $\angle(v_1v_2, w_2w_1) = \theta/2$ . The second case is that  $\angle(v_1v_2, w_2w_1) = -\theta/2$ . Consider a point  $p$  in extended  $\mathcal{T}_\phi$ .  $p$  can be a normal point or an auxiliary point.

Consider that  $\angle(v_1v_2, w_2w_1) = \theta/2$ . First, suppose  $w_1$  is the partition point and  $\phi$  is on the right side of  $v_1v_2$ . See Figure 23a. Suppose  $q$  belongs to  $\mathcal{T}_\varphi$  and  $\varphi \prec \phi$  (i.e.,  $q = q^{(1)}$  in Figure 23a). Denote the partition point in  $\mathcal{A}_\phi$  closest to  $w_2$  by  $\xi$ . Because of the projection of points in  $\mathcal{T}_\varphi$ ,  $\xi$  has two auxiliary points, denoted by  $\xi_1$  and  $\xi_2$ . Thus,  $pq$  is not an edge in the Yao-step since  $\xi_1$  and  $q$  are in the same cone of  $p$ . Then consider that  $q$  belongs to  $\mathcal{T}_\varphi$  and  $\varphi \succ \phi$  (i.e.,  $q = q^{(2)}$  in Figure 23a). Denote the point in  $\mathcal{B}_\phi$  closest to  $w_1$  by  $\eta$ . According to the fact that  $w_1\eta$  is the maximum length pair among the child-pairs of  $\phi$  (see Corollary 12),  $\eta$  and  $q$  are in the same cone of  $p$  when  $\angle(v_1v_2, pq) > 0$ . Thus, there is no long range connection for  $p$  in cone  $C_p(0, \theta]$ .

Second, suppose  $w_1$  is the apex point and  $\phi$  is on the left side of  $v_1v_2$ . See Figure 23b. Denote the closest point in  $\mathcal{B}_\phi$  to  $w_2$  by  $\eta$ . Suppose  $q$  belongs to  $\mathcal{T}_\varphi$  and  $\varphi \prec \phi$  (i.e.,  $q = q^{(1)}$  in Figure 23b). Because of the projection of points in  $\mathcal{T}_\varphi$ ,  $\eta$  has two auxiliary points, denoted by  $\eta_1$  and  $\eta_2$ . There is no edge  $pq$  in the Yao-step since  $\eta_1$  and  $q$  are in the same cone  $p$  and  $|\eta_1p| < |qp|$ . Then consider that  $q$  belongs to  $\mathcal{T}_\varphi$

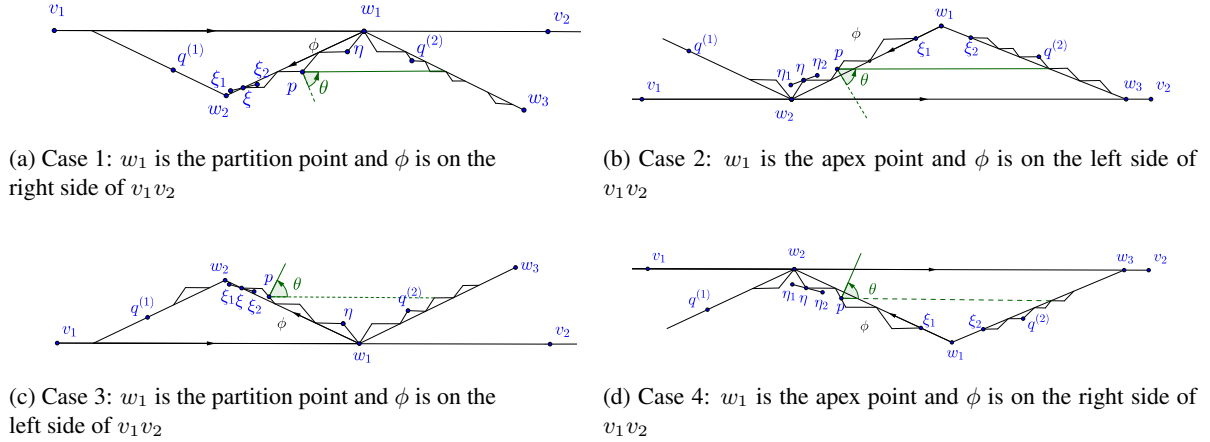


Figure 23: Here  $\phi = (w_1, w_2)$  and  $p$  belongs to the extended  $\mathcal{T}_\phi$  which includes auxiliary points.

and  $\varphi \succ \phi$  (i.e.,  $q = q^{(2)}$  in Figure 23b). If  $q$  in the cone  $C_p(0, \theta]$ ,  $q$  and  $w_1$  are in the same cone of  $p$  and  $|pw_1| < |pq|$ . Thus, in the Yao-step, there is no edge from  $p$  to  $q$  in the cone  $C_p(0, \theta]$ . Combining with Lemma 18, we prove the lemma in this case.

Then, we consider the case  $\angle(v_1v_2, w_2w_1) = -\theta/2$ . First, we consider the case in which  $w_1$  is the partition point and  $\phi$  is on the left side of  $v_1v_2$ . See Figure 23c. Denote the partition point in  $\mathcal{A}_\phi$  closest to  $w_2$  by  $\xi$ . According to the construction for auxiliary point (case 2a), we add two auxiliary points  $\xi_1$  and  $\xi_2$ . If  $q$  is in  $\mathcal{T}_\varphi$  and  $\varphi \prec \phi$  (i.e.,  $q = q^{(1)}$  in Figure 23c),  $\xi_1$  and  $q$  are in the same cone of  $p$  since the distance  $|\xi\xi_1| > \sigma^\kappa\chi^{-1}$ . Thus,  $pq$  is not an edge in the Yao-step since  $|\xi_1p| < |pq|$ . Then consider that  $q$  (i.e.,  $q = q^{(2)}$ ) in Figure 23c is in  $\mathcal{T}_\varphi$  and  $\varphi \succ \phi$ . If  $\angle(v_1v_2, pq) \in [-\theta/2, 0]$ ,  $pq$  is not a directed edge in Yao-step since  $w_1$  and  $q$  are in the same cone and  $|w_1p| < |pq|$ .

Finally, we consider the case that  $w_1$  is the apex point and  $\phi$  is on the right side of  $v_1v_2$ . Suppose  $\eta$  is the apex point in  $\mathcal{B}_\phi$  closest to  $w_2$ .  $\eta_1$  and  $\eta_2$  are auxiliary points of  $\eta$ . If  $q$  is in  $\mathcal{T}_\varphi$  and  $\varphi \prec \phi$  (i.e.,  $q = q^{(1)}$  in Figure 23d),  $\eta_1$  and  $q$  are in the same cone of  $p$  according to the construction for auxiliary point (case 2b). Thus,  $pq$  is not an edge in the Yao-step since  $|p\eta_1| < |pq|$ . Then consider  $q$  is in  $\mathcal{T}_\varphi$  and  $\varphi \succ \phi$  (i.e.,  $q = q^{(2)}$  in Figure 23d). If the polar angle of  $pq$  belongs to  $(-\theta, 0]$ ,  $w_1$  and  $q$  are in the same cone. Thus, there is no edge from  $p$  to  $q$  since  $|pq| > |pw_1|$ . Combining with Lemma 19, we prove the lemma in this case.

Overall, we have proved the lemma.  $\square$

Then, we prove that after adding the auxiliary points, there is no long range connection.

**Lemma 24.** *There is no long range connection in  $\mathcal{YY}_{2k+1}(\mathcal{P}_m)$ .*

*Proof.* Consider a pair  $(v_1, v_2)$  and a set  $\Phi$  of its child-pairs. Suppose  $\phi, \varphi \in \Phi$  and  $\varphi \prec \phi$ . According to Lemma 23 and Lemma 18 and 19, there is no directed edge from a point in extended  $\mathcal{T}_\phi$  to extended  $\mathcal{T}_\varphi$ .  $p$  is a point in  $\mathcal{T}_\varphi$ . Denote an auxiliary point centered on  $p$ , if any, by  $\xi$ . Let  $u \in \{p, \xi\}$ . There exists a point  $q$  closest to  $p$  such that  $q \in \mathcal{T}_\phi$  and  $pq$  is parallel to  $v_1v_2$ . If not, according to Lemma 23, there is no long range connection between  $u$  and points in extended  $\mathcal{T}_\phi$ . According to  $q$  is in  $\mathcal{A}_\phi \cup \mathcal{B}_\phi$  or  $\phi$ , there are two cases.

**$q$  is in  $\mathcal{A}_\phi \cup \mathcal{B}_\phi$ :**  $q$  has two auxiliary points  $\eta_1$  and  $\eta_2$  because of  $pq$ . Note that  $q$  may have a third auxiliary point  $\eta_3$ . But  $p$  and  $\eta_3$  are on the two different sides of  $\eta_1\eta_2$  and  $|\eta_3q| > |\eta_1q| = |\eta_2q|$  because of Property 22[P5]. Therefore, there is no directed edge  $p\eta_3$  in the Yao-step because  $\eta_2$  and  $\eta_3$  are in the same cone of  $p$  and  $|\eta_2p| < |\eta_3p|$ . According to Property 22[P4],  $|\xi p|$  is much less than  $|\eta_1q|$  or  $|\eta_2q|$

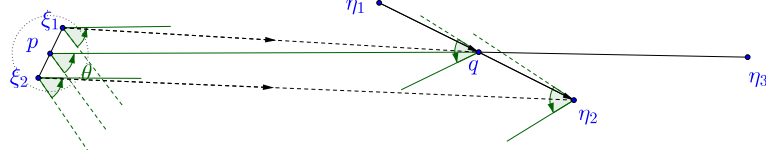
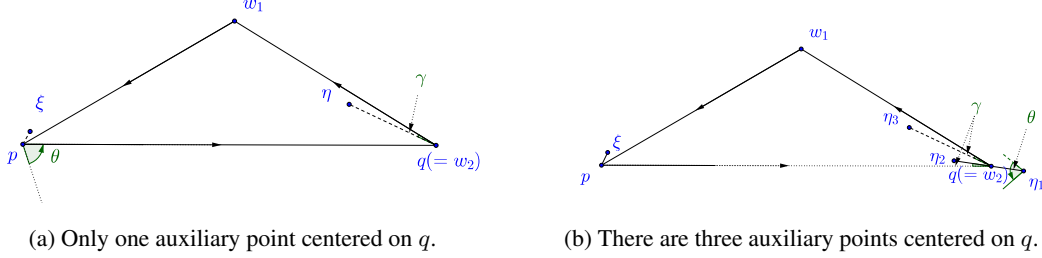


Figure 24: The case that  $q \in \mathcal{A}_\phi \cup \mathcal{B}_\phi$ .  $q$  may have three auxiliary points  $\{\eta_1, \eta_2, \eta_3\}$ .  $\xi_1$  and  $\xi_2$  are two possible positions of the auxiliary point  $\xi$  centered on  $p$ .



(a) Only one auxiliary point centered on  $q$ .

(b) There are three auxiliary points centered on  $q$ .

Figure 25:  $q$  is a point of pair  $\phi$ , i.e.,  $q = w_2$ .

and the perpendicular distance from  $\eta_1$  and  $\eta_2$  to the line  $pq$  is longer than  $|\xi p|$ . Suppose  $u \in \{p, \xi\}$ . See Figure 24 that is an enlarged view of Figure 22, in which  $\xi_1$  and  $\xi_2$  are two possible positions of  $\xi$ . According to Lemma 23,  $w\eta_1$  does not exist in the Yao-step since  $\eta_1$  and one point of  $\phi$  (denoted by  $w_1$ , refer to Figure 22) are in the same cone of  $u$  and  $|w_1 u| < |\eta_1 u|$ . If there is an edge  $u\eta_2$  in the Yao-step, the edge  $u\eta_2$  cannot be accepted by  $\eta_2$  in the reverse-Yao step since  $\eta_1 q$  exists, and point  $q$  and  $u$  are in the same cone of  $q$  and  $|q\eta_2| < |u\eta_2|$ . If there is an edge  $uq$  in the Yao-step, the edge  $uq$  cannot be accepted by  $q$  in the reverse-Yao step since  $\eta_1$  and  $u$  are in the same cone and  $|\eta_1 q| < |uq|$ . Therefore, there is no long range connection related to  $p$  and its auxiliary points.

**$q$  is a point of  $\phi$ :** See Figure 25. Note that in this case,  $q$  is point  $w_2$  of  $\phi$ . According to Property 22[P3], any point has at most three auxiliary points. Since  $q$  is a projection point of  $p$ ,  $q$  has at least one auxiliary point. Thus, there are two possible situations. One is that there is only one auxiliary point centered on  $q$  (see Figure 25a). It means that in the first time that  $q$  was able to be a candidate center,  $q$  is not a candidate center (see the proof of Property 22[P2]). Denote the auxiliary point of  $q$  by  $\eta$ . Let  $u \in \{p, \xi\}$  where  $\xi$  is an auxiliary point centered on  $p$ . According to the Property 22[P4],  $\eta$  and  $w_1$  are in the same cone of  $u$  and  $|uw_1| < |u\eta|$ . Therefore, there is no edge  $u\eta$  in the Yao-step. Moreover,  $uq$  cannot be accepted in the reverse-Yao step. Because the edge  $\eta q$  exists in the Yao-step.  $u$  and  $\eta$  are in the same cone of  $q$  and  $|\eta q| < |uq|$ . Combining with Lemma 23, there is no long range connection from  $u$  to  $\mathcal{T}_\phi$ . The second case is that there are three auxiliary points of  $q$  (see Figure 25b). Denote the auxiliary points of  $q$  by  $\{\eta_1, \eta_2, \eta_3\}$ . According to Property 22[P5], we know  $\angle \eta_2 q \eta_3 = (\theta/2 - 2\gamma)$ . Again, denote  $u \in \{p, \xi\}$ . There is no edge  $u\eta_3$  in the Yao-step since  $w_1$  and  $\eta_3$  are in the same cone of  $u$  and  $|uw_1| < |u\eta_3|$ . There is no edge  $u\eta_1$  in the reverse-Yao step, since there is an edge  $q\eta_1$  in the Yao-step and  $|q\eta_1| < |u\eta_1|$ . Similarly, there is no edge  $uq$  since there is an edge  $\eta_2 q$  in the Yao-step and  $|\eta_2 q| < |uq|$ . Next, note that  $|q\eta_2| \leq \sigma^{-1}|q\eta_3|$ . According to Property 22[P5], we know  $\eta_3$  and  $u$  are in the same cone of  $\eta_2$ . Thus, there is no edge from  $u\eta_2$ .

Overall, we prove that there is no long range connection in  $\mathbb{Y}\mathbb{Y}_{2k+1}(\mathcal{P}_m)$ .  $\square$

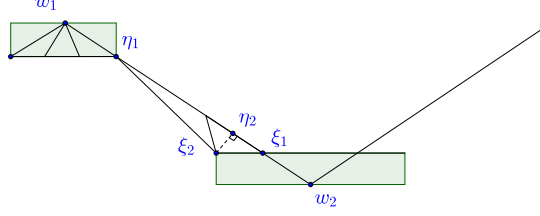


Figure 26: The shortest Euclidean distance between two hinge sets centered on points of a pair at  $level-(m-1)$ .

## 6 The Length Between $\mu_1$ and $\mu_2$ in $YY_{2k+1}(\mathcal{P}_m)$

In this section, we prove that the length of the shortest path between the initial points  $\mu_1$  and  $\mu_2$  in  $YY_{2k+1}(\mathcal{P}_m)$  diverges as  $m$  approaches infinity.

First, recall that we have generalized the concept of hinge sets to *extended hinge sets* which consist of the normal points in the hinge set and the auxiliary points of these normal points. Consider two extended hinge sets  $\Lambda$  and  $\Lambda'$ . Define the shortest path between  $\Lambda$  and  $\Lambda'$  to be the shortest path in  $YY_{2k+1}(\mathcal{P}_m)$  between any two points  $p$  and  $q$  such that  $p \in \Lambda$  and  $q \in \Lambda'$ . Consider any pair  $\phi = (w_1, w_2)$  at  $level-(m-1)$ . We give a lower bound on the shortest path distance between its former extended hinge set and latter extended hinge set.

**Lemma 25.** *Consider any pair  $(w_1, w_2)$  on  $level-(m-1)$ . Denote its former extended hinge set by  $\Lambda_\phi^{(-)}$ , and latter extended hinge set by  $\Lambda_\phi^{(+)}$ . The shortest path distance between  $\Lambda_\phi^{(-)}$  and  $\Lambda_\phi^{(+)}$  is at least  $(1 - 6d_0^{-1})|w_1w_2|$ .*

*Proof.* Let  $|w_1w_2| = \delta$ . See Figure 26. Note that the two hinge sets of  $w_1$  and  $w_2$  are not overlapping. Denote the near-empty piece incident on  $w_1$  by  $w_1\eta_1$  and the empty piece incident on  $w_2$  by  $w_2\xi_1$ .  $\xi_1\xi_2$  is the leaf-pair closest to  $w_2$ .  $\xi_2\eta_2$  is perpendicular to  $w_1w_2$ . The shortest Euclidean distance between the two hinge sets is no less than  $|\eta_1\eta_2|$ . According to Property 13,  $|w_1\eta_1| \leq 2d_0^{-1}\delta$ ,  $|w_2\xi_1| \leq d_0^{-1}\delta$  and  $\xi_1\eta_2 \leq 0.5d_0^{-1}\delta$ . Thus,  $|\eta_1\eta_2| > (1 - 3.5d_0^{-1})\delta$ .

Then consider the auxiliary points. Note that according to the Property 22[P1], the maximum distance between an auxiliary point and its center is  $d_0^{-1}\Delta$ , where  $\Delta$  is the minimum distance between any two normal points. Since  $\Delta \leq \delta$ , according to triangle inequality, the auxiliary points can reduce the distance between the two hinge sets at most  $2d_0^{-1}\delta$ . Overall, the shortest path between  $\Lambda_\phi^{(-)}$  and  $\Lambda_\phi^{(+)}$  is at least  $(1 - 6d_0^{-1})|w_1w_2|$ .  $\square$

According to Lemma 24, there is no long range connection in  $YY_{2k+1}(\mathcal{P}_m)$ . Thus, the shortest path between  $\mu_1$  and  $\mu_2$  should pass through all hinge sets in order. Thus, for each pair  $\phi$  at  $level-(m-1)$ , there is a path between  $\Lambda_\phi^{(-)}$  and  $\Lambda_\phi^{(+)}$ .

Let the shortest path between  $\Lambda_\phi^{(-)}$  and  $\Lambda_\phi^{(+)}$  be  $\Delta_\phi$ . Then, we prove that the sum of lengths of  $\Delta_\phi$  over all pairs at  $level-(m-1)$  diverges as  $m$  approaches infinity. Thus, the length of the shortest path between  $\mu_1$  and  $\mu_2$  diverges too.

**Lemma 26.** *The length of the shortest path between  $\mu_1$  and  $\mu_2$  in  $YY_{2k+1}(\mathcal{P}_m)$  for  $k \geq 3$  is at least  $\rho^m$ , for some  $\rho = (1 - O(d_0^{-1})) \cdot \cos^{-1}(\theta/2)$ . Thus, by setting  $d_0 = \Omega((1 - \cos(\theta/2))^{-1})$ , the length diverges as  $m$  approaches infinity.*

*Proof.* We give a lower bound of the sum of lengths  $|w_1 w_2|$  over all pairs  $(w_1, w_2)$  at *level*  $(m - 1)$ . Recall that the length of a pair is the length of the segment between the two points of the pair. Consider any pair  $\phi = (v_1, v_2)$  with length  $\delta$ . According to Property 13, the sum of lengths of half-empty, near-empty and empty pieces is no more than  $6d_0^{-1}\delta$ . Thus, the pieces which generate internal-pairs in next level have length at least  $(1 - 6d_0^{-1})\delta$ . For each piece, it generates two child-pairs. The sum of lengths of the two pairs is  $\cos^{-1}(\theta/2)$  times larger than the piece itself. Overall, the sum of the lengths of the pairs in generated next levels is at least  $(1 - 6d_0^{-1})\delta \cos^{-1}(\theta/2)$ . Let  $\rho = (1 - 6d_0^{-1}) \cos^{-1}(\theta/2)$ . Thus, after  $(m - 1)$  rounds, the length of the pairs at *level*  $(m - 1)$  is at least  $\rho^{m-1}|\mu_1 \mu_2|$ . According to Lemma 25, the shortest path from  $\mu_1$  to  $\mu_2$  is at least  $(1 - 6d_0^{-1})\rho^{m-1}|\mu_1 \mu_2|$ . When  $d_0 > 6(1 - \cos(\theta/2))^{-1}$ , the shortest path between  $\mu_1$  and  $\mu_2$  in  $\mathcal{YY}_{2k+1}(\mathcal{P}_m)$  diverges as  $m$  approaches infinity.  $\square$

Finally, combining with the results that  $\mathcal{YY}_3$  [13] and  $\mathcal{YY}_5$  [2] may not be spanners, we have proved Theorem 4.

**Theorem 4** (restated). *For any  $k \geq 1$ , there exists a class of instances  $\{\mathcal{P}_m\}_{m \in \mathbb{Z}^+}$  such that the stretch factor of  $\mathcal{YY}_{2k+1}(\mathcal{P}_m)$  cannot be bounded by any constant, as  $m$  approaches infinity.*

## References

- [1] AURENHAMMER, F. Voronoi diagrams a survey of a fundamental geometric data structure. *ACM Computing Surveys (CSUR)* 23, 3 (1991), 345–405.
- [2] BARBA, L., BOSE, P., DAMIAN, M., FAGERBERG, R., KENG, W. L., O’ROURKE, J., VAN RENSSSEN, A., TASLAKIAN, P., VERDONSCHOT, S., AND XIA, G. New and improved spanning ratios for Yao graphs. *JoCG* 6, 2 (2015), 19–53.
- [3] BARBA, L., BOSE, P., DE CARUFEL, J.-L., VAN RENSSSEN, A., AND VERDONSCHOT, S. On the stretch factor of the theta-4 graph. In *Workshop on Algorithms and Data Structures* (2013), Springer, pp. 109–120.
- [4] BAUER, M., AND DAMIAN, M. An infinite class of sparse-Yao spanners. In *Proceedings of the Twenty-Fourth Annual ACM-SIAM Symposium on Discrete Algorithms* (2013), SIAM, pp. 184–196.
- [5] BONICHON, N., GAVOILLE, C., HANUSSE, N., AND ILCINKAS, D. Connections between theta-graphs, delaunay triangulations, and orthogonal surfaces. In *International Workshop on Graph-Theoretic Concepts in Computer Science* (2010), Springer, pp. 266–278.
- [6] BOSE, P., DAMIAN, M., DOUÏEB, K., O’ROURKE, J., SEAMONE, B., SMID, M., AND WUHRER, S.  $\pi/2$ -angle Yao graphs are spanners. *International Journal of Computational Geometry & Applications* 22, 01 (2012), 61–82.
- [7] BOSE, P., MAHESHWARI, A., NARASIMHAN, G., SMID, M., AND ZEH, N. Approximating geometric bottleneck shortest paths. *Computational Geometry* 29, 3 (2004), 233–249.
- [8] BOSE, P., MORIN, P., VAN RENSSSEN, A., AND VERDONSCHOT, S. The  $\theta_5$ -graph is a spanner. *Computational Geometry* 48, 2 (2015), 108–119.
- [9] CHEW, P. There is a planar graph almost as good as the complete graph. In *Proceedings of the second annual symposium on Computational geometry* (1986), ACM, pp. 169–177.
- [10] DAMIAN, M. A simple Yao-Yao-based spanner of bounded degree. *arXiv preprint arXiv:0802.4325* (2008).

- [11] DAMIAN, M., MOLLA, N., AND PINCIU, V. Spanner properties of  $\pi/2$ -angle Yao graphs. In *Proc. of the 25th European Workshop on Computational Geometry* (2009), Citeseer, pp. 21–24.
- [12] DAMIAN, M., AND RAUDONIS, K. Yao graphs span theta graphs. In *Combinatorial Optimization and Applications*. Springer, 2010, pp. 181–194.
- [13] EL MOLLA, N. M. Yao spanners for wireless ad hoc networks. Master’s thesis, Villanova University, 2009.
- [14] EPPSTEIN, D. Spanning trees and spanners. *Handbook of computational geometry* (1999), 425–461.
- [15] EPPSTEIN, D. Beta-skeletons have unbounded dilation. *Computational Geometry* 23, 1 (2002), 43–52.
- [16] FLINCHBAUGH, B., AND JONES, L. Strong connectivity in directional nearest-neighbor graphs. *SIAM Journal on Algebraic Discrete Methods* 2, 4 (1981), 461–463.
- [17] GABRIEL, K. R., AND SOKAL, R. R. A new statistical approach to geographic variation analysis. *Systematic Biology* 18, 3 (1969), 259–278.
- [18] GRÜNEWALD, M., LUKOVSKI, T., SCHINDELHAUER, C., AND VOLBERT, K. Distributed maintenance of resource efficient wireless network topologies. In *European Conference on Parallel Processing* (2002), Springer, pp. 935–946.
- [19] JIA, L., RAJARAMAN, R., AND SCHEIDELER, C. On local algorithms for topology control and routing in ad hoc networks. In *Proceedings of the fifteenth annual ACM symposium on Parallel algorithms and architectures* (2003), ACM, pp. 220–229.
- [20] KANJ, I. A., AND XIA, G. On certain geometric properties of the Yao-Yao graphs. In *Combinatorial Optimization and Applications*. Springer, 2012, pp. 223–233.
- [21] LI, J., AND ZHAN, W. Almost all even yao-yao graphs are spanners. *The 24rd Annual European Symposium on Algorithms* (2016).
- [22] LI, X.-Y. *Wireless Ad Hoc and Sensor Networks: Theory and Applications*. Cambridge, 6 2008.
- [23] LI, X.-Y., WAN, P.-J., AND WANG, Y. Power efficient and sparse spanner for wireless ad hoc networks. In *Computer Communications and Networks, 2001. Proceedings. Tenth International Conference on* (2001), IEEE, pp. 564–567.
- [24] LI, X.-Y., WAN, P.-J., WANG, Y., AND FRIEDER, O. Sparse power efficient topology for wireless networks. In *System Sciences, 2002. HICSS. Proceedings of the 35th Annual Hawaii International Conference on* (2002), IEEE, pp. 3839–3848.
- [25] NARASIMHAN, G., AND SMID, M. *Geometric spanner networks*. Cambridge University Press, 2007.
- [26] RUPPERT, J., AND SEIDEL, R. Approximating the d-dimensional complete euclidean graph. In *Proceedings of the 3rd Canadian Conference on Computational Geometry (CCCG 1991)* (1991), pp. 207–210.
- [27] SACK, J.-R., AND URRUTIA, J. *Handbook of computational geometry*. Elsevier, 1999.
- [28] SCHINDELHAUER, C., VOLBERT, K., AND ZIEGLER, M. Spanners, weak spanners, and power spanners for wireless networks. In *International Symposium on Algorithms and Computation* (2004), Springer, pp. 805–821.

- [29] SCHINDELHAUER, C., VOLBERT, K., AND ZIEGLER, M. Geometric spanners with applications in wireless networks. *Computational Geometry* 36, 3 (2007), 197–214.
- [30] TOUSSAINT, G. T. The relative neighbourhood graph of a finite planar set. *Pattern recognition* 12, 4 (1980), 261–268.
- [31] WANG, Y., LI, X.-Y., AND FRIEDER, O. Distributed spanners with bounded degree for wireless ad hoc networks. *International Journal of Foundations of Computer Science* 14, 02 (2003), 183–200.
- [32] YAO, A. C.-C. On constructing minimum spanning trees in k-dimensional spaces and related problems. *SIAM Journal on Computing* 11, 4 (1982), 721–736.